A linear sampling method for near-field inverse problems in elastodynamics

Sylvain Nintcheu Fata and Bojan B Guzina

Department of Civil Engineering, University of Minnesota, Minneapolis, MN 55455, USA

E-mail: snintcheu@fata.ce.umn.edu and guzina@wave.ce.umn.edu

Abstract
The problem of reconstructing underground obstacles from near-field, surface seismic measurements is investigated within the framework of a linear sampling method. Although the latter approach has been the subject of mounting attention in inverse acoustics dealing with far-field wave patterns in infinite domains, there have apparently not been any attempts to apply this new method to the interpretation of near-field elastic wave forms such as those relevant to the detection of subterranean objects. Aimed at closing this gap, a three-dimensional inverse analysis of elastic waves scattered by an obstacle (or a system thereof), manifest in the surface ground motion patterns, is formulated as a linear integral equation of the first kind whose solution becomes unbounded in the exterior of the hidden scatterer. To provide a comprehensive theoretical foundation for this class of imaging solutions, generalization of the linear sampling method to near-field elastodynamics and semi-infinite domains is highlighted in terms of its key aspects. A set of numerical examples is included to illustrate the performance of the method. On replacing the featured elastodynamic half-space Green function by its free-space counterpart, the proposed study is directly applicable to infinite media as well.

(Some figures in this article are in colour only in the electronic version)

1. Introduction

Noninvasive identification of subterranean obstacles using elastic waves with frequencies in the resonance region is a long-standing problem in mechanics and engineering driven by its relevance to exploration seismology, nondestructive material testing, environmental remediation, medical diagnosis and defence applications. For this class of inverse scattering problems, employed imaging solutions are often based on nonlinear optimization which requires an initial approximation of the geometry and topology of the scattering obstacle [18, 28, 35, 38].

Over the past decade, developments in sonar and radar technologies have led to the introduction of an alternative technique for solving inverse scattering problems in the resonance region called the *linear sampling method*. Originally proposed by Colton *et al* in a series of papers [7, 8, 12, 13] for far-field acoustics, the linear sampling method furnishes an explicit characterization of a hidden obstacle (provided that the far-field pattern is known for all directions of incidence and observation), and is independent of geometry and physical properties of the scattering object. To date, this new technique has been adapted to electromagnetics [10, 11, 25] and to far-field elastic scattering problems [2–4, 20, 37].

Although the linear sampling method has received considerable attention in inverse scattering theory dealing with far-field wave patterns in the free space, limited attention has so far been paid to its application involving near-field elastic wave forms, especially those arising in the half-space during active seismic imaging of underground obstacles (e.g., defence facilities, buried waste and land mines). In particular, application of the former sonar and radar solutions to seismic imaging has been impeded not only by the inherent heterogeneity of geological profiles, but also by the fact that elastic waves, unlike their acoustic counterpart, take many different forms (compressional, shear, Love, Rayleigh and Stoneley waves, see [1, 21]), which renders their interpretation challenging. Aimed at bridging such a gap, this investigation focuses on establishing a rigorous theoretical framework for the identification of hidden obstacles in a uniform elastic half-space via the linear sampling method. To this end, a three-dimensional inverse analysis of elastic waves scattered by a buried object, manifest in the surface ground motion patterns, is formulated as a linear integral equation of the first kind whose solution becomes unbounded in the exterior of an unknown scatterer. The generalization of the linear sampling method to near-field elastodynamics and semi-infinite domains is highlighted, including the necessary existence and uniqueness theorems. Illustrative examples with ellipsoidal cavities are included to provide an insight into the performance of the method.

2. Direct scattering problem

With reference to the Cartesian frame $\{O; \xi_1, \xi_2, \xi_3\}$ shown in figure 1, consider the scattering of time-harmonic elastic waves by a bounded obstacle Ω_C with boundary Γ of class $C^{1,\alpha}$, $\alpha \in (0, 1]$, strictly embedded in a homogeneous elastic half-space $\Omega = \{(\xi_1, \xi_2, \xi_3)|\xi_3 > 0\}$. The semi-infinite 'matrix' domain Ω is characterized by the Lamé constants λ and μ, mass density ρ; its free surface $\{(\xi_1, \xi_2, \xi_3)|\xi_3 = 0\}$ is denoted by S. For further reference, let $\Omega^- = \Omega \setminus (\Omega_C \cup \Gamma)$ denote the unbounded region surrounding the obstacle, and let ω be the frequency of excitation.

With the time-harmonic factor $e^{i\omega t}$ omitted henceforth for brevity, the incident (or free) field $\boldsymbol{u}^{Fk}(\cdot, \boldsymbol{\zeta})$ used to illuminate the scatterer is generated by a point source acting on a planar surface $\Gamma_1 \subset S$ of finite extent so that

$$\boldsymbol{u}^{Fk}(\boldsymbol{\xi}, \boldsymbol{\zeta}) = \hat{\boldsymbol{u}}^k(\boldsymbol{\xi}, \boldsymbol{\zeta}), \qquad \boldsymbol{\xi} \neq \boldsymbol{\zeta}, \qquad \boldsymbol{\xi} \in \Omega, \qquad \boldsymbol{\zeta} \in \Gamma_1, \qquad (1)$$

where $\hat{\boldsymbol{u}}^k(\boldsymbol{\xi}, \boldsymbol{\zeta})$ denotes the elastodynamic displacement Green function for an isotropic homogeneous half-space at $\boldsymbol{\xi} \in \Omega$ due to a unit time-harmonic point force acting at $\boldsymbol{\zeta} \in \Gamma_1$ in the kth coordinate direction. By denoting the total displacement field at $\boldsymbol{\xi} \in \Omega^-$ due to a unit point source acting at $\boldsymbol{\zeta} \in \Gamma_1$ in the kth coordinate direction by $\boldsymbol{u}^k(\boldsymbol{\xi}, \boldsymbol{\zeta})$, one can define the scattered field $\boldsymbol{u}^{Sk}(\boldsymbol{\xi}, \boldsymbol{\zeta})$ through the decomposition

$$\boldsymbol{u}^{Sk}(\boldsymbol{\xi}, \boldsymbol{\zeta}) = \boldsymbol{u}^k(\boldsymbol{\xi}, \boldsymbol{\zeta}) - \boldsymbol{u}^{Fk}(\boldsymbol{\xi}, \boldsymbol{\zeta}), \qquad \boldsymbol{\xi} \in \Omega^-, \qquad \boldsymbol{\zeta} \in \Gamma_1. \qquad (2)$$
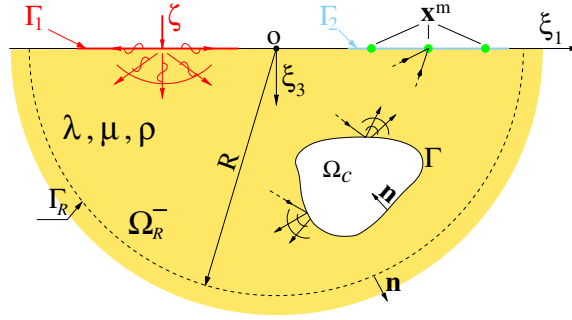
Figure 1. Point source excitation of an obstacle embedded in the half-space.

With reference to any smooth surface Σ in Ω with unit normal $\boldsymbol{n}$, it is instructive to introduce the traction vector $\boldsymbol{t}(\cdot\,; \boldsymbol{u})$ associated with a displacement vector $\boldsymbol{u}$ as

$$\boldsymbol{t}(\boldsymbol{\xi}; \boldsymbol{u}) = \boldsymbol{n}(\boldsymbol{\xi}) \cdot \mathbf{C} : \nabla \boldsymbol{u}(\boldsymbol{\xi}), \qquad \boldsymbol{\xi} \in \Sigma, \tag{3}$$

where $\mathbf{C} = \lambda \mathbf{I}_2 \otimes \mathbf{I}_2 + 2\mu \mathbf{I}_4$ denotes the isotropic elasticity tensor and $\mathbf{I}_k$ $(k = 2, 4)$ is the symmetric kth order identity tensor.

  With such definitions, the forward elastodynamic problem for an obstacle Ω_C can be formulated as a task of finding the scattered field $\boldsymbol{u}^{Sk} \in C^2(\Omega^-) \cap C^1(\Omega^- \cup \Gamma \cup S)$ that satisfies the homogeneous Navier equation

$$\boldsymbol{L} \boldsymbol{u}^{Sk}(\boldsymbol{\xi}, \boldsymbol{\zeta}) + \rho \omega^2 \boldsymbol{u}^{Sk}(\boldsymbol{\xi}, \boldsymbol{\zeta}) = \mathbf{0}, \qquad \boldsymbol{\xi} \in \Omega^-, \quad \boldsymbol{\zeta} \in \Gamma_1, \tag{4}$$

with the Lamé operator $\boldsymbol{L}$ defined as

$$\boldsymbol{L} = \mu \nabla^2 + (\lambda + \mu) \nabla \nabla \cdot, \tag{5}$$

and boundary conditions

$$
\begin{aligned}
\boldsymbol{t}^{Sk}(\boldsymbol{\xi}, \boldsymbol{\zeta}) &= \mathbf{0}, & \boldsymbol{\xi} &\in S, \quad \boldsymbol{\zeta} \in \Gamma_1, & \\
\boldsymbol{u}^{Sk}(\boldsymbol{\xi}, \boldsymbol{\zeta}) &= -\boldsymbol{u}^{Fk}(\boldsymbol{\xi}, \boldsymbol{\zeta}), & \boldsymbol{\xi} &\in \Gamma, \quad \boldsymbol{\zeta} \in \Gamma_1 & \text{if } \Omega_C \text{ is an immobile rigid body,} \\
\boldsymbol{t}^{Sk}(\boldsymbol{\xi}, \boldsymbol{\zeta}) &= -\boldsymbol{t}^{Fk}(\boldsymbol{\xi}, \boldsymbol{\zeta}), & \boldsymbol{\xi} &\in \Gamma, \quad \boldsymbol{\zeta} \in \Gamma_1 & \text{if } \Omega_C \text{ is a cavity.}
\end{aligned}
\tag{6}
$$

In (4) through (6), the free field $\boldsymbol{u}^{Fk}$ is provided beforehand, while $\boldsymbol{t}^{Fk}$ and $\boldsymbol{t}^{Sk}$ are the traction vectors associated, respectively, with $\boldsymbol{u}^{Fk}$ and $\boldsymbol{u}^{Sk}$ on $\Gamma \cup S$. To maintain the well posedness of the forward scattering problem, it is assumed that $\boldsymbol{u}^{Sk}$ conforms with the generalized radiation condition

$$\lim_{R \to \infty} \int_{\Gamma_R} \{\hat{\boldsymbol{u}}^j(\boldsymbol{\xi}, \boldsymbol{x}) \cdot \boldsymbol{t}^{Sk}(\boldsymbol{\xi}, \boldsymbol{\zeta}) - \hat{\boldsymbol{t}}^j(\boldsymbol{\xi}, \boldsymbol{x}) \cdot \boldsymbol{u}^{Sk}(\boldsymbol{\xi}, \boldsymbol{\zeta})\} \, \mathrm{d}\Gamma_{\boldsymbol{\xi}} = 0, \qquad \boldsymbol{x} \in \Omega_R^-, \quad j = 1, 2, 3, \tag{7}$$

where $\hat{\boldsymbol{t}}^j(\boldsymbol{\xi}, \boldsymbol{x})$ is the traction vector at $\boldsymbol{\xi} \in \Gamma_R$ associated with $\hat{\boldsymbol{u}}^j(\boldsymbol{\xi}, \boldsymbol{x})$, namely the half-space traction Green's function; Γ_R is a hemisphere centred at the origin O, and Ω_R^- is the subset of Ω^- bounded by Γ_R (see figure 1).

  A solution to (4) that satisfies (7) is called a radiating solution of the homogeneous Navier equation in Ω^-. In what follows, it is assumed that the forward scattering problem for the semi-infinite solid Ω^- given by (4), (6) and (7) admits a unique solution $\boldsymbol{u}^{Sk} \in H^1_{\mathrm{loc}}(\Omega^-)$, see [27].

3. Inverse scattering problem

To formulate the inverse problem of elastic waves scattered by an obstacle Ω_C within the framework of near-field elastodynamics, let $\widehat{U}(\xi, \zeta)$ denote the half-space displacement Green tensor at $\xi \in \Omega\backslash\{\zeta\}$ due to a unit point source acting at $\zeta \in \Gamma_1$. In a Cartesian frame, $\widehat{U}(\xi, \zeta)$ can be synthesized via a 3×3 matrix as

$$\widehat{U}(\xi, \zeta) = \left(\hat{u}^1(\xi, \zeta), \hat{u}^2(\xi, \zeta), \hat{u}^3(\xi, \zeta)\right) = \begin{pmatrix} \hat{u}_1{}^1(\xi, \zeta) & \hat{u}_1{}^2(\xi, \zeta) & \hat{u}_1{}^3(\xi, \zeta) \\ \hat{u}_2{}^1(\xi, \zeta) & \hat{u}_2{}^2(\xi, \zeta) & \hat{u}_2{}^3(\xi, \zeta) \\ \hat{u}_3{}^1(\xi, \zeta) & \hat{u}_3{}^2(\xi, \zeta) & \hat{u}_3{}^3(\xi, \zeta) \end{pmatrix}. \tag{8}$$

In what follows, the vector field $u(x, z; d) = \widehat{U}(x, z) \cdot d$ defines the displacement at $x \in \Omega\backslash\{z\}$ due to a unit point source at z acting in the direction specified by the unit vector d ($d \in \mathbb{R}^3$, $\|d\| = 1$). Owing to the symmetry of the half-space displacement Green functions [23], one can write

$$\left[\widehat{U}(\zeta, \xi)\right]^{\mathrm{T}} = \widehat{U}(\xi, \zeta), \tag{9}$$

where the superscript 'T' stands for matrix transpose. To aid the ensuing development, it is also useful to establish the scattered tensor $U^{\mathrm{S}}(\xi, \zeta)$ at $\xi \in \Omega^-$ due to a unit point source acting at $\zeta \in \Gamma_1$ through

$$U^{\mathrm{S}}(\xi, \zeta) = (u^{\mathrm{S}1}(\xi, \zeta), u^{\mathrm{S}2}(\xi, \zeta), u^{\mathrm{S}3}(\xi, \zeta)) = \begin{pmatrix} u_1^{\mathrm{S}1}(\xi, \zeta) & u_1^{\mathrm{S}2}(\xi, \zeta) & u_1^{\mathrm{S}3}(\xi, \zeta) \\ u_2^{\mathrm{S}1}(\xi, \zeta) & u_2^{\mathrm{S}2}(\xi, \zeta) & u_2^{\mathrm{S}3}(\xi, \zeta) \\ u_3^{\mathrm{S}1}(\xi, \zeta) & u_3^{\mathrm{S}2}(\xi, \zeta) & u_3^{\mathrm{S}3}(\xi, \zeta) \end{pmatrix} \tag{10}$$

in Cartesian coordinates. In what follows, U^{S} will be used to synthesize the experimental data collected over the observation surface $\Gamma_2 \subset S$. In the case of incomplete measurements of the scattered field, the corresponding columns of U^{S} in (10) are set to zero. For instance, if $u^{\mathrm{S}3}$ is the only quantity being monitored (i.e. only vertical point sources are used to illuminate the scatterer), then the first and second columns of U^{S} in (10) are set to zero.

With the above definitions, the inverse scattering problem of interest in this study can be set forth as a task of reconstructing Ω_C from the knowledge of the tensor of scattered displacement field components $U^{\mathrm{S}}(\xi, \zeta)$ for all observation points $\xi \in \Gamma_2 \subset S$ and all source points $\zeta \in \Gamma_1 \subset S$. Inverse scattering problems of this type are inherently nonlinear and improperly posed. In particular, unless regularization methods are used, small perturbations of the observed (i.e. measured) data $U^{\mathrm{S}}(\xi, \zeta)$ in any reasonable norm may lead to large errors in the reconstruction of the scatterer [13].

4. Preliminaries

The linear sampling method, originally introduced by Colton and Kirsch [7] for far-field inverse scattering problems in acoustics, will be used in this study to tackle the featured inverse problem within the framework of near-field elastodynamics. To aid such a generalization, let $L_2(S_1)$ be the Hilbert space of square integrable vector fields equipped with the inner product

$$(g, h)_{L_2(S_1)} = \int_{S_1} \overline{g}(x) \cdot h(x) \, \mathrm{d}s_x, \tag{11}$$

where the overbar denotes complex conjugation. Further, with reference to any smooth surface Σ in Ω with unit normal $\boldsymbol{n}$, let the half-space traction Green tensor $\widehat{\boldsymbol{T}}(\boldsymbol{\xi}, \boldsymbol{\zeta})$ at $\boldsymbol{\xi} \in \Sigma$ due to a unit point source acting at $\boldsymbol{\zeta} \in \Gamma_1$ be denoted as

$$\widehat{\boldsymbol{T}}(\boldsymbol{\xi}, \boldsymbol{\zeta}) = \boldsymbol{n}(\boldsymbol{\xi}) \cdot \mathbf{C} : \nabla \widehat{\boldsymbol{U}}(\boldsymbol{\xi}, \boldsymbol{\zeta}) := \begin{pmatrix} \hat{t}_1{}^1(\boldsymbol{\xi}, \boldsymbol{\zeta}) & \hat{t}_1{}^2(\boldsymbol{\xi}, \boldsymbol{\zeta}) & \hat{t}_1{}^3(\boldsymbol{\xi}, \boldsymbol{\zeta}) \\ \hat{t}_2{}^1(\boldsymbol{\xi}, \boldsymbol{\zeta}) & \hat{t}_2{}^2(\boldsymbol{\xi}, \boldsymbol{\zeta}) & \hat{t}_2{}^3(\boldsymbol{\xi}, \boldsymbol{\zeta}) \\ \hat{t}_3{}^1(\boldsymbol{\xi}, \boldsymbol{\zeta}) & \hat{t}_3{}^2(\boldsymbol{\xi}, \boldsymbol{\zeta}) & \hat{t}_3{}^3(\boldsymbol{\xi}, \boldsymbol{\zeta}) \end{pmatrix} \tag{12}$$

in the reference Cartesian frame.

Theorem 4.1. *Let S_1 be a surface of limited extent of class $C^{1,\alpha}$ in Ω and $\boldsymbol{g} \in L_2(S_1)$. Then a single layer potential*

$$\boldsymbol{v}(\boldsymbol{\xi}) = \int_{S_1} \widehat{\boldsymbol{U}}(\boldsymbol{\xi}, \boldsymbol{x}) \cdot \boldsymbol{g}(\boldsymbol{x}) \, \mathrm{d}s_{\boldsymbol{x}} = \int_{S_1} \hat{u}^k(\boldsymbol{\xi}, \boldsymbol{x}) g_k(\boldsymbol{x}) \, \mathrm{d}s_{\boldsymbol{x}}, \qquad \boldsymbol{\xi} \in \Omega \setminus S_1 \tag{13}$$

is a radiating solution to the homogeneous Navier equation in $\Omega \setminus S_1$, i.e.

$$\boldsymbol{L}\boldsymbol{v}(\boldsymbol{\xi}) + \rho \omega^2 \boldsymbol{v}(\boldsymbol{\xi}) = \boldsymbol{0}, \qquad \boldsymbol{\xi} \in \Omega \setminus S_1, \tag{14}$$

and

$$\lim_{R \to \infty} \int_{\Gamma_R} \{\hat{u}^j(\boldsymbol{\xi}, \boldsymbol{x}) \cdot \boldsymbol{t}(\boldsymbol{\xi}; \boldsymbol{v}) - \hat{t}^j(\boldsymbol{\xi}, \boldsymbol{x}) \cdot \boldsymbol{v}(\boldsymbol{\xi})\} \, \mathrm{d}\Gamma_{\boldsymbol{\xi}} = 0, \qquad \boldsymbol{x} \in \Omega_R, \quad j = 1, 2, 3, \tag{15}$$

where $\boldsymbol{t}(\boldsymbol{\xi}; \boldsymbol{v}) = \boldsymbol{n}(\boldsymbol{\xi}) \cdot \mathbf{C} : \nabla \boldsymbol{v}(\boldsymbol{\xi})$ is the traction vector associated with the displacement field $\boldsymbol{v}$ on any regular surface in Ω with unit normal $\boldsymbol{n}$.

Proof. Since $\boldsymbol{\xi} \in \Omega \setminus S_1$, (13) can be differentiated under the integral sign and (14) follows directly from the fact that $\hat{u}^k$ ($k = 1, 2, 3$) satisfies the homogeneous Navier equation away from the source surface S_1.

By use of (12) in (13), one can deduce that

$$\boldsymbol{t}(\boldsymbol{\xi}; \boldsymbol{v}) = \int_{S_1} \widehat{\boldsymbol{T}}(\boldsymbol{\xi}, \boldsymbol{x}) \cdot \boldsymbol{g}(\boldsymbol{x}) \, \mathrm{d}s_{\boldsymbol{x}} = \int_{S_1} \hat{t}^k(\boldsymbol{\xi}, \boldsymbol{x}) g_k(\boldsymbol{x}) \, \mathrm{d}s_{\boldsymbol{x}}, \qquad \boldsymbol{\xi} \neq \boldsymbol{x} \tag{16}$$

on any regular surface in Ω with unit normal $\boldsymbol{n}$. On employing (13) and (16) and interchanging the order of integration, one can verify that

$$\int_{\Gamma_R} \{\hat{u}^j(\boldsymbol{\xi}, \boldsymbol{x}) \cdot \boldsymbol{t}(\boldsymbol{\xi}; \boldsymbol{v}) - \hat{t}^j(\boldsymbol{\xi}, \boldsymbol{x}) \cdot \boldsymbol{v}(\boldsymbol{\xi})\} \, \mathrm{d}\Gamma_{\boldsymbol{\xi}}$$
$$= \int_{S_1} g_k(\boldsymbol{x}) \left(\int_{\Gamma_R} \{\hat{t}^k(\boldsymbol{\xi}, \boldsymbol{y}) \cdot \hat{u}^j(\boldsymbol{\xi}, \boldsymbol{x}) - \hat{t}^j(\boldsymbol{\xi}, \boldsymbol{x}) \cdot \hat{u}^k(\boldsymbol{\xi}, \boldsymbol{y})\} \, \mathrm{d}\Gamma_{\boldsymbol{\xi}} \right) \mathrm{d}s_{\boldsymbol{x}}. \tag{17}$$

The statement (15) immediately follows from (17), and the fact that the half-space displacement Green function $\hat{u}^k(\cdot, \boldsymbol{z})$ ($k = 1, 2, 3$) is a radiating solution to the homogeneous Navier equation in $\Omega \setminus \{\boldsymbol{z}\}$, see [23]. $\qquad \square$

The following lemma will be very useful in establishing the linear sampling method.

Lemma 4.1. *For a given density distribution $\boldsymbol{g} \in L_2(\Gamma_1)$, the solution to the scattering problem by an obstacle Ω_C in the half-space Ω due to the free field*

$$\boldsymbol{v}^{\mathrm{F}}(\boldsymbol{\xi}) = \int_{\Gamma_1} \widehat{\boldsymbol{U}}(\boldsymbol{\xi}, \boldsymbol{x}) \cdot \boldsymbol{g}(\boldsymbol{x}) \, \mathrm{d}s_{\boldsymbol{x}}, \qquad \boldsymbol{\xi} \in \Omega \setminus \Gamma_1 \tag{18}$$

is given by the scattered field

$$\boldsymbol{v}^{\mathrm{S}}(\boldsymbol{\xi}) = \int_{\Gamma_1} \boldsymbol{U}^{\mathrm{S}}(\boldsymbol{\xi}, \boldsymbol{x}) \cdot \boldsymbol{g}(\boldsymbol{x}) \, \mathrm{d}s_{\boldsymbol{x}} = \int_{\Gamma_1} u^{\mathrm{S}k}(\boldsymbol{\xi}, \boldsymbol{x}) g_k(\boldsymbol{x}) \, \mathrm{d}s_{\boldsymbol{x}}, \qquad \boldsymbol{\xi} \in \Omega^-, \tag{19}$$

where $\widehat{\boldsymbol{U}}$ and $\boldsymbol{U}^{\mathrm{S}}$ are defined, respectively, by (8) and (10).

Proof. An integral representation for the scattered field u^{Sk} (e.g., [36]) in terms of the total displacement field u^k and the total traction t^k over the obstacle boundary $\partial\Omega_C = \Gamma$ due to a point source $x \in \Gamma_1$ in the kth coordinate direction is given by

$$
u^{Sk}(\xi, x) = \int_\Gamma [\widehat{U}(\eta, \xi)]^T \cdot t^k(\eta, x) \, d\Gamma_\eta
$$
$$
- \int_\Gamma [\widehat{T}(\eta, \xi)]^T \cdot u^k(\eta, x) \, d\Gamma_\eta, \qquad \begin{matrix} \xi \in \Omega^- \\ x \in \Gamma_1. \end{matrix} \tag{20}
$$

On using (20) in (19) and interchanging the order of integration, one finds that

$$
v^S(\xi) = \int_\Gamma [\widehat{U}(\eta, \xi)]^T \cdot t(\eta; v) \, d\Gamma_\eta - \int_\Gamma [\widehat{T}(\eta, \xi)]^T \cdot v(\eta) \, d\Gamma_\eta, \qquad \xi \in \Omega^-, \tag{21}
$$

where

$$
v(\xi) = \int_{\Gamma_1} u^k(\xi, x) g_k(x) \, ds_x, \qquad \xi \in \Omega^-, \tag{22}
$$

and $t(\eta; v) = n(\eta) \cdot C : \nabla v(\eta)$ as examined earlier. It is seen from (21) that $v^S(\xi)$ admits a representation similar to (20) in terms of a single-layer potential

$$
P(\xi) = \int_\Gamma [\widehat{U}(\eta, \xi)]^T \cdot t(\eta; v) \, d\Gamma_\eta, \qquad \xi \in \Omega^-, \tag{23}
$$

and a double-layer potential

$$
Q(\xi) = \int_\Gamma [\widehat{T}(\eta, \xi)]^T \cdot v(\eta) \, d\Gamma_\eta, \qquad \xi \in \Omega^-. \tag{24}
$$

Following the idea of the proof of theorem 4.1, one can show that P and Q are radiating solutions of the homogeneous Navier equation in Ω^-. From this statement and the linearity of (21) (i.e. $v^S = P - Q$), one can infer that v^S is also a radiating solution of the homogeneous Navier equation in Ω^-. Now, with the aid of (1) and (2) in (22), it is seen that $v = v^F(\xi) + v^S(\xi), \xi \in \Omega^-$ where v^F and v^S are given, respectively, by (18) and (19). $\qquad \square$

Before establishing the linear sampling method for near-field elastodynamics, one should mention that lemma 4.1 is a reformulation, suitable for elastic scattering problems, of lemma 3.16 in [9] for inverse acoustics.

5. Linear sampling method

On the basis of the foregoing developments, one is now in a position to formulate the linear sampling method for elastic-wave reconstruction of the scatterer Ω_C hidden in a semi-infinite solid from the knowledge of scattered field along the observation surface Γ_2 synthesized via the tensor $U^S(\xi, x), \xi \in \Gamma_2, x \in \Gamma_1$ (see (10) and figure 1). The underlying idea is to find a free field v^F with density g over the source surface Γ_1 so that the corresponding scattered field v^S (see lemma 4.1) coincides with a prescribed radiating solution to the homogeneous Navier equation in Ω^- which, in particular, is chosen as the displacement $\widehat{U}(\cdot, z) \cdot d, \|d\| = 1$, due to a point source acting at $z \in \Omega$ in the direction d.

In mathematical terms, let $z \in \Omega$ be fixed. The objective is to find the vector density $g_{z,d}(\cdot) \equiv g(\cdot; z, d) \in L_2(\Gamma_1)$ as a solution to the near-field integral equation of the first kind

$$
\int_{\Gamma_1} U^S(\xi, x) \cdot g_{z,d}(x) \, ds_x = \widehat{U}(\xi, z) \cdot d, \qquad \xi \in \Omega^-, \quad z \in \Omega, \quad d \in \mathbb{R}^3, \quad \|d\| = 1. \tag{25}
$$

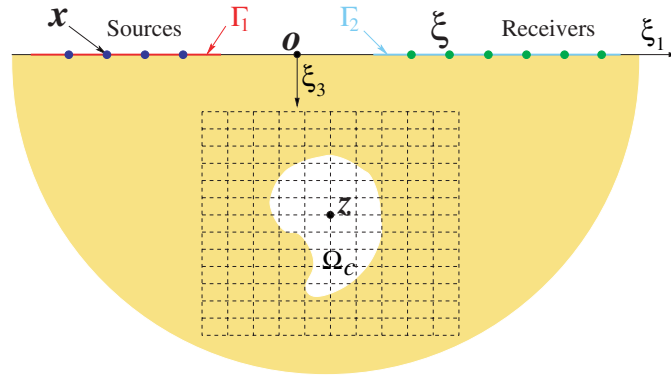**Figure 2.** Probing grid of sample points.

Let $z \in \Omega_C$. On employing (19) and taking the limit as $\xi \to y \in \Gamma$ in (25), one can write

$$v^S(y) = \widehat{U}(y, z) \cdot d, \qquad y \in \Gamma, \quad z \in \Omega_C, \quad d \in \mathbb{R}^3, \quad \|d\| = 1. \tag{26}$$

Letting $z \to y \in \Gamma$ in (26), one finds that $v^S(y)$ becomes unbounded, and, since U^S is bounded on Γ, one must have $\lim_{z \to y \in \Gamma} \|g(\cdot; z, d)\|_{L_2(\Gamma_1)} = \infty$, where $\|g\|_{L_2(\Gamma_1)} = \sqrt{(g, g)_{L_2(\Gamma_1)}}$. For completeness, it will also be shown in this study that $\|g(\cdot; z, d)\|_{L_2(\Gamma_1)}$ becomes unbounded whenever $z \in \Omega^-$. As a result, the *unboundedness* property of $g(\cdot; z, d)$ can be used to reconstruct the unknown scatterer Ω_C. The key idea is to sample a region of interest in the half-space Ω by varying the probing (i.e. sampling) point z, and to identify Ω_C (if any) through a location of those sampling points z where $\|g(\cdot; z, d)\|_{L_2(\Gamma_1)}$ is bounded.

In practical terms, the scattered tensor U^S is assumed to be measured on a bounded planar subdomain Γ_2 of the surface of the half-space S (see figure 2) so that the following specialization of (25)

$$\int_{\Gamma_1} U^S(\xi, x) \cdot g_{z,d}(x) \, ds_x = \widehat{U}(\xi, z) \cdot d, \qquad \xi \in \Gamma_2, \quad z \in \Omega, \quad d \in \mathbb{R}^3, \quad \|d\| = 1 \tag{27}$$

needs to be solved for the density $g_{z,d}$.

The above formulation of the linear sampling method for solving inverse scattering problems is, despite its elegance, fraught with difficulties. One should mention that equation (27) constitutes a Fredholm integral equation of the first kind with a smooth kernel given by the scattered tensor field U^S synthesizing experimental observations. Since solving Fredholm integral equations of this type is an improperly posed mathematical problem in the sense of Hadamard [26], it is not clear whether a solution $g_{z,d}$ to (27) exists and, if such a solution does exist, whether $g_{z,d}$ depends continuously on the measured data U^S in any reasonable norm. Thus, a mathematical justification of the linear sampling method is necessary to consistently deal with these impediments.

6. Theoretical foundation

To extend the linear sampling method to near-field inverse elastic scattering problems, one has to analyse the near-field Fredholm integral equation of the first kind (27) in order to justify the method. The case where $z \in \Omega_C$ is first considered, wherein the necessary existence and uniqueness theorems in terms of density $g_{z,d}$ that characterizes the scatterer Ω_C are

established. As mentioned in section 2, it is assumed that a unique solution $u^{Sk} \in H^1_{loc}(\Omega^-)$ to the direct scattering problem (4) to (7) exists.

The following basic identities of the mathematical theory of linear elasticity will be of great importance in the subsequent development. Let D be a bounded elastic domain (characterized by an isotropic elastic tensor $\mathbf{C}$) with boundary ∂D of class $C^{1,\alpha}$, and let $\boldsymbol{n}$ denote the unit outward normal to ∂D. Then, for vector fields $\boldsymbol{u}, \boldsymbol{v} \in C^2(D) \cap C^1(\overline{D})$, Betti's first formula, obtained by integration by parts, takes the form

$$\int_D \boldsymbol{v}(\xi) \cdot \boldsymbol{L}\boldsymbol{u}(\xi) \, \mathrm{d}V_\xi = \int_{\partial D} \boldsymbol{v}(\xi) \cdot \boldsymbol{t}(\xi; \boldsymbol{u}) \, \mathrm{d}s_\xi - \int_D \nabla \boldsymbol{v}(\xi) : \mathbf{C} : \nabla \boldsymbol{u}(\xi) \, \mathrm{d}V_\xi, \tag{28}$$

where the Lamé operator $\boldsymbol{L}$ is given by (5) and $\boldsymbol{t}(\xi; \boldsymbol{u}) = \boldsymbol{n}(\xi) \cdot \mathbf{C} : \nabla \boldsymbol{u}(\xi)$ as elucidated earlier. By setting $\boldsymbol{v} = \boldsymbol{u}$ in (28), Betti's second formula can be expressed as

$$\int_D \boldsymbol{u}(\xi) \cdot \boldsymbol{L}\boldsymbol{u}(\xi) \, \mathrm{d}V_\xi = \int_{\partial D} \boldsymbol{u}(\xi) \cdot \boldsymbol{t}(\xi; \boldsymbol{u}) \, \mathrm{d}s_\xi - \int_D \nabla \boldsymbol{u}(\xi) : \mathbf{C} : \nabla \boldsymbol{u}(\xi) \, \mathrm{d}V_\xi. \tag{29}$$

On interchanging the role of $\boldsymbol{u}$ and $\boldsymbol{v}$ in (28) and subtracting the latter from (28), one can write Betti's third formula as

$$\int_D [\boldsymbol{v}(\xi) \cdot \boldsymbol{L}\boldsymbol{u}(\xi) - \boldsymbol{u}(\xi) \cdot \boldsymbol{L}\boldsymbol{v}(\xi)] \, \mathrm{d}V_\xi = \int_{\partial D} [\boldsymbol{v}(\xi) \cdot \boldsymbol{t}(\xi; \boldsymbol{u}) - \boldsymbol{u}(\xi) \cdot \boldsymbol{t}(\xi; \boldsymbol{v})] \, \mathrm{d}s_\xi. \tag{30}$$

To aid the ensuing development, the following *near-field* operator $\boldsymbol{F} : L_2(\Gamma_1) \to L_2(\Gamma_2)$ defined as

$$(\boldsymbol{F}\boldsymbol{g})(\xi) := \int_{\Gamma_1} \boldsymbol{U}^S(\xi, \boldsymbol{x}) \cdot \boldsymbol{g}(\boldsymbol{x}) \, \mathrm{d}s_{\boldsymbol{x}}, \qquad \xi \in \Gamma_2 \tag{31}$$

is also introduced where Γ_1 and Γ_2 are, respectively, the surfaces of source and observation points, while $\boldsymbol{U}^S$ is the scattered tensor given by (10). One should note that for $\boldsymbol{U}^S \in L_2(\Gamma_2 \times \Gamma_1)$, the operator $\boldsymbol{F}$ is well defined, linear and bounded from $L_2(\Gamma_1)$ into $L_2(\Gamma_2)$. The latter property can be seen from the inequality

$$\|\boldsymbol{F}\boldsymbol{g}\|^2_{L_2(\Gamma_2)} \leqslant \|\boldsymbol{g}\|^2_{L_2(\Gamma_1)} \left(\sum_{k=1}^3 \sum_{j=1}^3 \int_{\Gamma_2} \int_{\Gamma_1} \left| u^{Sk}_j(\xi, \boldsymbol{x}) \right|^2 \mathrm{d}s_{\boldsymbol{x}} \, \mathrm{d}s_\xi \right) \tag{32}$$

obtained using the Cauchy–Schwarz inequality [29], where $|\cdot|$ is the complex modulus. It can also be shown [29] that the linear integral operator $\boldsymbol{F}$ is *compact* from $L_2(\Gamma_1)$ into $L_2(\Gamma_2)$, thus rendering the linear equation (27) ill-posed.

In what follows, the solvability condition for the integral equation of the first kind (27) when $z \in \Omega_C$ is given in terms of the following theorem, derived by analogy to its acoustic counterpart (theorem 3.19 in [9]).

Theorem 6.1. *Let $z \in \Omega_C$ be fixed. Then the integral equation of the first kind*

$$\int_{\Gamma_1} \boldsymbol{U}^S(\xi, \boldsymbol{x}) \cdot \boldsymbol{g}_{z,d}(\boldsymbol{x}) \, \mathrm{d}s_{\boldsymbol{x}} = \widehat{\boldsymbol{U}}(\xi, z) \cdot \boldsymbol{d}, \qquad \xi \in \Gamma_2, \quad z \in \Omega_C, \quad \boldsymbol{d} \in \mathbb{R}^3, \quad \|\boldsymbol{d}\| = 1 \tag{33}$$

possesses a solution $\boldsymbol{g}_{z,d} \in L_2(\Gamma_1)$ if and only if there exists a solution $\boldsymbol{v}^F$ to the interior boundary value problem given by

$$\boldsymbol{L}\boldsymbol{v}^F(\xi) + \rho\omega^2 \boldsymbol{v}^F(\xi) = \boldsymbol{0}, \qquad \xi \in \Omega_C, \tag{34}$$

$$\boldsymbol{v}^F(\xi) + \widehat{\boldsymbol{U}}(\xi, z) \cdot \boldsymbol{d} = \boldsymbol{0}, \qquad \xi \in \Gamma, \tag{35}$$

for the scattering by an immovable rigid inclusion (Dirichlet problem), and by

$$Lv^{\mathrm{F}}(\xi) + \rho\omega^2 v^{\mathrm{F}}(\xi) = \mathbf{0}, \qquad \xi \in \Omega_{\mathrm{C}}, \tag{36}$$

$$t(\xi; v^{\mathrm{F}}) + \widehat{T}(\xi, z) \cdot d = \mathbf{0}, \qquad \xi \in \Gamma, \tag{37}$$

for the scattering by a cavity (the Neumann problem), that is expressible in the form of (18), where $t(\cdot; v^{\mathrm{F}})$ denotes the traction vector associated with v^{F}.

Proof. Let $g_{z,d} \in L_2(\Gamma_1)$ be a solution to (33) and define v^{F} according to (18) by

$$v^{\mathrm{F}}(\xi) = \int_{\Gamma_1} \widehat{U}(\xi, x) \cdot g_{z,d}(x)\,\mathrm{d}s_x, \qquad \xi \in \Omega \backslash \Gamma_1. \tag{38}$$

Then, from lemma 4.1,

$$v^{\mathrm{S}}(\xi) = \int_{\Gamma_1} U^{\mathrm{S}}(\xi, x) \cdot g_{z,d}(x)\,\mathrm{d}s_x, \qquad \xi \in \Omega^- \tag{39}$$

is a radiating solution to the homogeneous Navier equation in Ω^-. Since z is held fixed in Ω_{C}, one can infer that $\widehat{U}(\xi, z) \cdot d, \xi \in \Omega^-$ is also a radiating solution to the homogeneous Navier equation in Ω^- (see theorem 2.2.1 in [34]), and by use of (33), that $v^{\mathrm{S}}(\xi) = \widehat{U}(\xi, z) \cdot d$ on Γ_2. With the aid of the latter result and Holmgren's uniqueness theorem [6, 17], one can conclude that, in fact

$$v^{\mathrm{S}}(\xi) = \widehat{U}(\xi, z) \cdot d, \qquad \xi \in \Omega^-. \tag{40}$$

For the scattering by an immobile rigid obstacle, one has

$$v^{\mathrm{F}}(\xi) + v^{\mathrm{S}}(\xi) = \mathbf{0}, \qquad \xi \in \Gamma. \tag{41}$$

On substituting the limit of (40) as $\xi \to y \in \Gamma$ into (41), one obtains (35). For scattering by a cavity, on the other hand,

$$t(\xi; v^{\mathrm{F}}) + t(\xi; v^{\mathrm{S}}) = \mathbf{0}, \qquad \xi \in \Gamma. \tag{42}$$

From (40), the traction vector $t(\xi; v^{\mathrm{S}})$ (associated with v^{S}) on any surface strictly inside Ω^- with unit normal n is given by $\widehat{T}(\xi, z) \cdot d$, which, in the limit as $\xi \to y \in \Gamma$, (42) yields (37). Further, since the source surface Γ_1 is away from the scatterer Ω_{C}, (34) (or (36)) directly follows from theorem 4.1.

Conversely, let $v^{\mathrm{F}}(\xi)$ be a solution of (34) and (35) (or (36) and (37)). Then $v^{\mathrm{F}}(\xi)$ can be taken as a free field for scattering by an obstacle Ω_{C} and, from lemma 4.1, the unique radiating solution, u^{S}, to this scattering problem is given by (39) with boundary condition (41) (or (42)). Comparison of (35) and (41) (or (37) and (42)) yields

$$v^{\mathrm{S}}(\xi) = \widehat{U}(\xi, z) \cdot d, \qquad (\text{or } t(\xi; v^{\mathrm{S}}) = \widehat{T}(\xi, z) \cdot d), \qquad \xi \in \Gamma. \tag{43}$$

Holmgren's uniqueness theorem can again be used to obtain (40) and the proof follows by taking the limit as $\xi \to y \in \Gamma_2$. $\qquad\square$

6.1. Approximation property of single-layer potentials

One of the key issues in establishing the validity of the linear sampling method for inverse scattering problems dealing with *far-field* observations is concerned with the approximation property of Herglotz wavefunctions (see, e.g., [14] for acoustics and [16] for elastodynamics). To facilitate the ensuing development, it is instructive to mention that the single-layer potential defining the free field $v^{\mathrm{F}}(\xi)$ in (18) plays the same role in this investigation as the Herglotz wavefunction does for the sampling method in far-field inverse acoustic or elastic scattering problems. Accordingly, the next step in this study is to establish the denseness property of single-layer potentials such as those characterizing v^{F}.

With the above settings, let $D \subset \Omega$ be a bounded domain with boundary ∂D of class $C^{1,\alpha}$ and let $\mathbb{H}(D)$ be the set of classical solutions to the homogeneous Navier equation in D, i.e.

$$\mathbb{H}(D) = \{\boldsymbol{u} \in C^2(D) \cap C^1(\overline{D}) : \boldsymbol{L}\boldsymbol{u} + \rho\omega^2\boldsymbol{u} = \boldsymbol{0} \text{ in } D\}.$$

From the above definition, it is readily shown that for any $\boldsymbol{u} \in \mathbb{H}(D)$, its complex conjugate belongs to the same space, i.e. $\overline{\boldsymbol{u}} \in \mathbb{H}(D)$ and thus

$$\overline{\boldsymbol{t}(\cdot; \boldsymbol{u})} = \boldsymbol{t}(\cdot; \overline{\boldsymbol{u}}), \qquad \boldsymbol{u} \in \mathbb{H}(D). \tag{44}$$

For further reference, let $L_2(D)$ be the Hilbert space of square integrable vector fields equipped with the usual inner product

$$(\boldsymbol{v}, \boldsymbol{u})_{L_2(D)} = \int_D \overline{\boldsymbol{v}}(\boldsymbol{\xi}) \cdot \boldsymbol{u}(\boldsymbol{\xi}) \, dV_\xi, \tag{45}$$

and $H^1(D) = \{\boldsymbol{u} \in L_2(D), \nabla\boldsymbol{u} \in L_2(D)\}$ be the Hilbert space equipped with the Hermitian product

$$(\boldsymbol{v}, \boldsymbol{u})_{H^1(D)} = \theta \int_D \overline{\boldsymbol{v}}(\boldsymbol{\xi}) \cdot \boldsymbol{u}(\boldsymbol{\xi}) \, dV_\xi + \int_D \nabla\overline{\boldsymbol{v}}(\boldsymbol{\xi}) : \boldsymbol{C} : \nabla\boldsymbol{u}(\boldsymbol{\xi}) \, dV_\xi, \qquad \mathbb{R} \ni \theta > 0, \tag{46}$$

and denote by $\overline{\mathbb{H}(D)}$ the closure of $\mathbb{H}(D)$ with the norm of $H^1(D)$ given by

$$\|\boldsymbol{u}\|_{H^1(D)} = \sqrt{(\boldsymbol{u}, \boldsymbol{u})_{H^1(D)}}. \tag{47}$$

Now, consider the single-layer integral operator $\boldsymbol{S} : L_2(\Gamma_1) \to \overline{\mathbb{H}(D)}$ defined by

$$(\boldsymbol{S}\boldsymbol{g})(\boldsymbol{\xi}) := \int_{\Gamma_1} \widehat{\boldsymbol{U}}(\boldsymbol{\xi}, \boldsymbol{x}) \cdot \boldsymbol{g}(\boldsymbol{x}) \, ds_x, \qquad \boldsymbol{\xi} \in D. \tag{48}$$

The operator $\boldsymbol{S}$ given by (48) is well defined. It is important first to mention that Γ_1 lies outside $\overline{D}$, i.e. $\Gamma_1 \cap \overline{D} = \emptyset$, and for that reason, $\boldsymbol{S}\boldsymbol{g} \in C^\infty(\overline{D}) \subset C^2(D) \cap C^1(\overline{D})$. But from theorem 4.1, the field $\boldsymbol{S}\boldsymbol{g}$ satisfies the homogeneous Navier equation in D and therefore $\boldsymbol{S}\boldsymbol{g} \in \mathbb{H}(D)$.

Lemma 6.1. *For all $\boldsymbol{g} \in L_2(\Gamma_1)$ and $\boldsymbol{u} \in \overline{\mathbb{H}(D)}$, the following identity holds*

$$(\boldsymbol{S}\boldsymbol{g}, \boldsymbol{u})_{L_2(D)} = (\boldsymbol{g}, \boldsymbol{S}_D^*\boldsymbol{u})_{L_2(\Gamma_1)}, \tag{49}$$

where $\boldsymbol{S}_D^* : \overline{\mathbb{H}(D)} \to L_2(\Gamma_1)$ is given by

$$(\boldsymbol{S}_D^*\boldsymbol{u})(\boldsymbol{x}) := \int_D \overline{\widehat{\boldsymbol{U}}(\boldsymbol{x}, \boldsymbol{\xi})} \cdot \boldsymbol{u}(\boldsymbol{\xi}) \, dV_\xi, \qquad \boldsymbol{x} \in \Gamma_1.$$

Proof. For $\boldsymbol{g} \in L_2(\Gamma_1)$ and $\boldsymbol{u} \in \mathbb{H}(D)$,

$$(\boldsymbol{S}\boldsymbol{g}, \boldsymbol{u})_{L_2(D)} = \int_D \boldsymbol{u}(\boldsymbol{\xi}) \cdot \left(\int_{\Gamma_1} \overline{\widehat{\boldsymbol{U}}(\boldsymbol{\xi}, \boldsymbol{x})} \cdot \overline{\boldsymbol{g}(\boldsymbol{x})} \, ds_x\right) dV_\xi. \tag{50}$$

On interchanging the order of integration in (50) and employing the symmetry of $\widehat{\boldsymbol{U}}$ in (9), it is seen that

$$(\boldsymbol{S}\boldsymbol{g}, \boldsymbol{u})_{L_2(D)} = \int_{\Gamma_1} \overline{\boldsymbol{g}(\boldsymbol{x})} \cdot \left(\int_D \overline{\widehat{\boldsymbol{U}}(\boldsymbol{x}, \boldsymbol{\xi})} \cdot \boldsymbol{u}(\boldsymbol{\xi}) \, dV_\xi\right) ds_x = (\boldsymbol{g}, \boldsymbol{S}_D^*\boldsymbol{u})_{L_2(\Gamma_1)}. \tag{51}$$

The statement of the lemma follows from the fact that $\mathbb{H}(D)$ is dense in $\overline{\mathbb{H}(D)}$. $\qquad\square$

Lemma 6.2. *For all $\boldsymbol{g} \in L_2(\Gamma_1)$ and $\boldsymbol{u} \in \overline{\mathbb{H}(D)}$, the following identity holds:*

$$(\boldsymbol{S}\boldsymbol{g}, \boldsymbol{u})_{H^1(D)} = (\boldsymbol{g}, \boldsymbol{S}^*\boldsymbol{u})_{L_2(\Gamma_1)}, \tag{52}$$
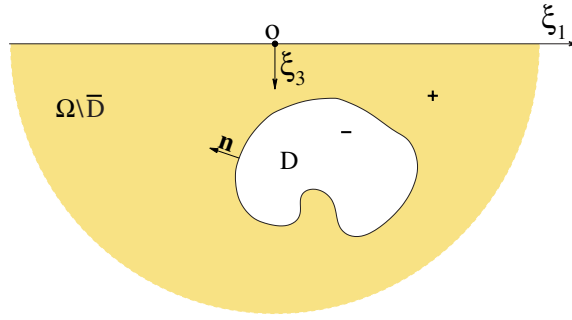
Figure 3. Interior and exterior domains.

where $S^* : \overline{\mathbb{H}(D)} \to L_2(\Gamma_1)$ is given by

$$(S^*u)(x) := (\theta + \rho\omega^2) \int_D \overline{\widehat{U}(x, \xi)} \cdot u(\xi) \, dV_\xi + \int_{\partial D} \overline{\widehat{U}(x, \xi)} \cdot t(\xi; u) \, ds_\xi, \qquad x \in \Gamma_1 \tag{53}$$

with the traction vector $t(\cdot; u) \in H^{-1/2}(\partial D)$ understood in the sense of the trace of $u \in H^1(D)$, see [33].

Proof. Let $g \in L_2(\Gamma_1)$; on the basis of the comment made right after the definition of S in (48), it follows that $Sg \in \mathbb{H}(D)$. Now let $u \in \mathbb{H}(D)$. Using Betti's first formula (28), the homogeneous Navier equation for the vector field u in D, and the sesquilinear form (46), one can write

$$(Sg, u)_{H^1(D)} = (\theta + \rho\omega^2)(Sg, u)_{L_2(D)} + (Sg, t(\cdot; u))_{L_2(\partial D)}. \tag{54}$$

Similar to the proof of lemma 6.1, one can derive the relationship (52) from (54) and the identity (49). The statement of the lemma again follows by the denseness argument. $\square$

For $u \in \overline{\mathbb{H}(D)}$, the adjoint operator S^*, defined through (53) as a linear combination of volume and surface potentials, can be used to introduce the vector field

$$\begin{aligned} v(x) &:= \overline{(S^*u)(x)} \\ &= (\theta + \rho\omega^2) \int_D \widehat{U}(x, \xi) \cdot \overline{u(\xi)} \, dV_\xi + \int_{\partial D} \widehat{U}(x, \xi) \cdot \overline{t(\xi; u)} \, ds_\xi, \qquad x \in \Omega \backslash \partial D. \end{aligned} \tag{55}$$

Using Lax's theorem [29], it can be shown that the volume potential in (55) is a bounded linear operator from $L_2(D)$ into $H^2_{loc}(\Omega)$ (see also [9]). Accordingly, since the single-layer potential in (55) is a bounded linear operator from $H^{-1/2}(\partial D)$ into $H^1_{loc}(\Omega \backslash \overline{D})$ (see [31]), one can conclude that the mapping $u \longmapsto v$ given by (55) defines a bounded linear operator from $H^1(D)$ into $H^1_{loc}(\Omega \backslash \overline{D})$. Since elastic potentials behave near boundaries much like ordinary harmonic potentials, it can be shown that

$$v(x) = v_+(x) = v_-(x), \qquad t_+(x; v) - t_-(x; v) = -\overline{t(x; u)}, \quad x \in \partial D, \tag{56}$$

where the subscripts '+' and '$-$' stand for the limiting values of the corresponding quantity at the boundary ∂D when approached, respectively, from the exterior domain $\Omega \backslash \overline{D}$ and from the interior domain D (see figure 3).

For $x \in D$, formula (55) can be differentiated under the integral sign. By taking into account that the support of the half-space displacement Green function $\hat{u}^k(x, \xi)$ is resting in D, i.e.

$$L\hat{u}^k(x, \xi) + \rho\omega^2\hat{u}^k(x, \xi) + \delta_{ki}\delta(x - \xi)e_i = 0, \qquad x \in D, \qquad (57)$$

where δ_{ki} is the Kronecker delta, $\delta(x - \xi)$ is the Dirac delta function and e_i is a unit vector in the ith coordinate direction, it can be shown that

$$Lv(x) + \rho\omega^2 v(x) = -(\theta + \rho\omega^2)\overline{u(x)}, \qquad x \in D. \qquad (58)$$

In what follows, it is assumed that $u \in \mathbb{H}(D)$. By use of the Navier equation for the field u in D and Betti's second formula (29) in (47), one can write

$$\|u\|^2_{H^1(D)} = (\theta + \rho\omega^2)\int_D \overline{u(\xi)} \cdot u(\xi)\,\mathrm{d}V_\xi + \int_{\partial D} \overline{u(\xi)} \cdot t(\xi; u)\,\mathrm{d}s_\xi. \qquad (59)$$

With the aid of (44), (56) and (58), (59) can be expressed as

$$\|u\|^2_{H^1(D)} = -\int_D \overline{u}(\xi) \cdot [L\overline{v}(\xi) + \rho\omega^2\overline{v}(\xi)]\,\mathrm{d}V_\xi - \int_{\partial D} \overline{u}(\xi) \cdot [t_+(\xi; \overline{v}) - t_-(\xi; \overline{v})]\,\mathrm{d}s_\xi. \qquad (60)$$

By use of Betti's third formula (30), the Navier equation for the field $\overline{u}$ in D and (44), it can be shown that (60) admits the following representation:

$$\|u\|^2_{H^1(D)} = \int_{\partial D} [v(\xi) \cdot t(\xi; u) - u(\xi) \cdot t_+(\xi; v)]\,\mathrm{d}s_\xi. \qquad (61)$$

With the above settings, one is now in position to formulate the following result.

Lemma 6.3. *For all* $u \in \overline{\mathbb{H}(D)}$,

$$\|u\|^2_{H^1(D)} = \int_{\partial D} [v(\xi) \cdot t(\xi; u) - u(\xi) \cdot t_+(\xi; v)]\,\mathrm{d}s_\xi, \qquad (62)$$

where $v \in H^1_{loc}(\Omega \backslash \overline{D})$ *is given by (55).*

Proof. The statement of the lemma readily follows from (61) for $u \in \mathbb{H}(D)$, and the denseness argument. $\qquad\square$

Theorem 6.2. *The space of single-layer potentials* $\{Sg, g \in L_2(\Gamma_1)\}$ *given by (48) is dense in the space of classical solutions to the homogeneous Navier equation:* $Lu + \rho\omega^2 u = 0$ *in D with respect to the $H^1(D)$ norm, i.e.* $S(L_2(\Gamma_1))$ *is dense with respect to the $H^1(D)$ norm in* $\overline{\mathbb{H}(D)}$.

Proof. Let $u \in \overline{\mathbb{H}(D)}$ and assume that $(Sg, u)_{H^1(D)} = 0$ for all $g \in L_2(\Gamma_1)$. Then, by lemma 6.2, one can write $(g, S^*u)_{L_2(\Gamma_1)} = 0$ for all $g \in L_2(\Gamma_1)$ and consequently $S^*u = 0$ (see (53)). Now, by making use of Holmgren's uniqueness theorem, one can conclude that $v = 0$ in Ω^-. Finally it follows from lemma 6.3 that $\|u\|_{H^1(D)} = 0$, hence $u = 0$ in D. $\qquad\square$

6.2. Mathematical validation

As mentioned in section 3, the linear sampling method for solving inverse scattering problems is based on the integral equation of the first kind (33) which, in general, does not possess a solution. In fact, (33) constitutes an improperly posed mathematical problem in the sense of Hadamard [26]. To examine the problem further, let F be the near-field operator as defined by (31). With the results of the preceding section, the fact that (33) is in general not solvable can be overcome with the following result.

Theorem 6.3 (Existence). *Let $z \in \Omega_C$ be fixed, $d \in \mathbb{R}^3$ with $\|d\| = 1$, and let Γ be of class $C^{1,\alpha}$. Then, for every $\varepsilon > 0$, there exists $g(\cdot; z, d) \in L_2(\Gamma_1)$ such that*

$$\|Fg(\cdot; z, d) - \widehat{U}(\cdot, z) \cdot d\|_{L_2(\Gamma_2)} < \varepsilon, \tag{63}$$

where

$$\lim_{z \to y \in \Gamma} \|g(\cdot; z, d)\|_{L_2(\Gamma_1)} = \infty, \tag{64}$$

and the single-layer potential $Sg(x; z, d)$ defined by (48) becomes unbounded as $z \to x \in \Gamma$.

Proof. Consider the interior boundary value problem given by

$$Lw(x) + \rho\omega^2 w(x) = 0, \qquad x \in \Omega_C, \tag{65}$$

$$w(x) + \widehat{U}(x, z) \cdot d = 0, \qquad x \in \Gamma, \quad z \in \Omega_C, \tag{66}$$

for the scattering by an immovable rigid inclusion (the Dirichlet problem), and by

$$Lw(x) + \rho\omega^2 w(x) = 0, \qquad x \in \Omega_C, \tag{67}$$

$$t(x; w) + \widehat{T}(x, z) \cdot d = 0, \qquad x \in \Gamma, \quad z \in \Omega_C, \tag{68}$$

for the scattering by a cavity (the Neumann problem) in terms of w. It follows from theorem 6.2 that the solution, w, to the Navier equation (65) (or 67) can be approximated arbitrarily well by a single-layer potential Sg with respect to the $H^1(\Omega_C)$ norm, i.e. for every $\varepsilon > 0$, there exists $g(\cdot; z, d) \in L_2(\Gamma_1)$ such that

$$\|w - Sg(\cdot; z, d)\|_{H^1(\Omega_C)} < c_0\varepsilon, \qquad \mathbb{R} \ni c_0 > 0. \tag{69}$$

Now, by virtue of the continuity of the norm, boundary conditions (66) and (68), and the trace theorem [33], there exist positive constants c_1 and c_2 such that

$$\|\widehat{U}(\cdot, z) \cdot d + Sg(\cdot; z, d)\|_{H^{1/2}(\Gamma)} < c_1\varepsilon,$$

for the scattering by an immobile rigid inclusion (the Dirichlet problem), and

$$\|\widehat{T}(\cdot, z) \cdot d + t(\cdot; Sg(\cdot; z, d))\|_{H^{-1/2}(\Gamma)} < c_2\varepsilon,$$

for the scattering by a cavity (the Neumann problem). The proof of (63) now follows by virtue of theorem 6.1.

With the above approximation property of the single-layer potential Sg and the trace theorem, there exist positive constants c and c' such that

$$\|\widehat{U}(\cdot, z) \cdot d\|_{H^{1/2}(\Gamma)} \leqslant c\|w\|_{H^1(\Omega_C)} \leqslant c(c_0\varepsilon + \|Sg(\cdot; z, d)\|_{H^1(\Omega_C)}), \tag{70}$$

$$\|\widehat{T}(\cdot, z) \cdot d\|_{H^{-1/2}(\Gamma)} \leqslant c'(c_0\varepsilon + \|Sg(\cdot; z, d)\|_{H^1(\Omega_C)}). \tag{71}$$

Since the single-layer integral operator S is bounded [34] from $L_2(\Gamma_1) \to H^1(\Omega_C)$ for $g(\cdot; z, d) \in L_2(\Gamma_1)$, there exists a constant $c'' > 0$ such that

$$\|Sg(\cdot; z, d)\|_{H^1(\Omega_C)} \leqslant c''\|g(\cdot; z, d)\|_{L_2(\Gamma_1)}. \tag{72}$$

With (70) to (72) and the limiting properties of the half-space Green functions

$$\lim_{z \to y \in \Gamma} \|\widehat{U}(\cdot, z) \cdot d\|_{H^{1/2}(\Gamma)} = \infty, \qquad \lim_{z \to y \in \Gamma} \|\widehat{T}(\cdot, z) \cdot d\|_{H^{-1/2}(\Gamma)} = \infty, \tag{73}$$

the second claim of the theorem (given by (64)) and the unboundedness of Sg immediately follow. $\qquad\square$

Remark. One may note that (73) is a consequence of the following reasoning: as $\Omega_C \ni z \to y \in \Gamma$, the radiating field $v(x, z) = \widehat{U}(x, z) \cdot d$ that satisfies the homogeneous Navier equation outside any ball containing z exhibits the singular behaviour

$$v(y, z) = O\left(\frac{1}{\|y - z\|}\right), \qquad \text{as } \|y - z\| \to 0 \tag{74}$$

owing to the singularity of the half-space displacement Green functions as $\|y - z\| \to 0$ (see [22]). In what follows, $v(\cdot, z) \notin H_{\text{loc}}^1(\Omega^-)$ since

$$\nabla v(y, z) = O\left(\frac{1}{\|y - z\|^2}\right), \qquad \text{as } \|y - z\| \to 0.$$

Hence, the restrictions of $v(x, z)$ on Γ given by $\widehat{U}(y, z) \cdot d$ and $\widehat{T}(y, z) \cdot d$, $y \in \Gamma$ are so that $\widehat{U}(\cdot, z) \cdot d \notin H^{1/2}(\Gamma)$ and $\widehat{T}(\cdot, z) \cdot d \notin H^{-1/2}(\Gamma)$.

Theorem 6.4 (Uniqueness). *The near-field operator $F : L_2(\Gamma_1) \to L_2(\Gamma_2)$ given by (31) is injective (one-to-one) if and only if there does not exists neither a Dirichlet nor a Neumann eigenfunction for the obstacle Ω_C that is a single-layer potential Sg defined by (48).*

Proof. The equation

$$Fg = 0 \tag{75}$$

is solvable (see theorem 6.1) if and only if the following interior boundary value problem

$$Lw(x) + \rho\omega^2 w(x) = 0, \qquad x \in \Omega_C, \tag{76}$$

with

$$w(x) = 0, \qquad x \in \Gamma, \tag{77}$$

for the Dirichlet problem and

$$t(x; w) = 0, \qquad x \in \Gamma, \tag{78}$$

for the Neumann problem, admits a solution. But (76) and (77) constitute the Dirichlet eigenvalue problem for $-L$ in Ω_C, while (76) and (78) are the Neumann eigenvalue problem for $-L$ in Ω_C. From theorem 6.2, w can be approximated arbitrarily well by a single-layer potential Sg with respect to the $H^1(\Omega_C)$ norm. Thus, the statement that (75) holds with $g \neq 0$ is equivalent to the existence of the Dirichlet (problem (76) and (77)) or Neumann ((76) and (78)) eigenfunction $w = Sg$ for Ω_C, which is in contradiction with the statement of the theorem and completes the proof. $\square$

Remark. One can infer from the result of the above theorem that the unboundedness property of g (see theorem 6.3) is not due to elements of the nullspace of F herein denoted by $\ker F$.

6.3. Reconstruction of an infinitesimal cavity

To investigate the performance of the linear sampling method for an obstacle of vanishing size, consider the elastic-wave reconstruction of a 'small' cavity hidden in the half-space Ω. Without loss of generality, it is assumed that the cavity, denoted as $B_\tau(z)$, is a ball of radius $\tau > 0$ centred at a fixed sampling point $z \in \Omega$. In this setting, one is to solve the equation

$$
\begin{aligned}
(F^\tau g_{z,d}^\tau)(\xi) &:= \int_{\Gamma_1} U_\tau^S(\xi, x) \cdot g_{z,d}^\tau(x) \, ds_x \\
&= \widehat{U}(\xi, z) \cdot d, \qquad \xi \in \Gamma_2, \quad d \in \mathbb{R}^3, \quad \|d\| = 1,
\end{aligned}
\tag{79}
$$

where $U_\tau^S(\xi, x)$ is the scattered tensor induced by $B_\tau(z) \subset \Omega$ at $\xi \in \Gamma_2$ due to a unit point source at $x \in \Gamma_1$. For a vanishing cavity size, it can be shown [24] that U_τ^S admits the representation

$$U_\tau^S(\xi, x) = -\frac{4\pi\tau^3}{3}(\rho\omega^2[\widehat{U}(z, \xi)]^T \cdot \widehat{U}(z, x) - \mathcal{M}(\xi, x)) + o(\tau^3), \qquad \text{as } \tau \to 0, \quad (80)$$

where $\mathcal{M}(\xi, x)$ is a 3×3 matrix with components $\mathcal{M}_i{}^k(\xi, x) = \hat{\sigma}^i(z, \xi) : \mathcal{A} : \hat{\sigma}^k(z, x)$ constructed from the elastodynamic stress Green tensor $\hat{\sigma}^k = \mathbf{C} : \nabla \hat{u}^k$, and

$$\mathcal{A} = \frac{3(\lambda + 2\mu)}{2\mu(9\lambda + 14\mu)} \left[5\mathbf{I}_4 - \frac{7\lambda + 2\mu}{2(3\lambda + 2\mu)} \mathbf{I}_2 \otimes \mathbf{I}_2 \right].$$

On employing (9) and neglecting higher order terms in (80), one can write

$$(\boldsymbol{F}^\tau \boldsymbol{g})(\xi) = -\frac{4\pi\tau^3}{3} \left[\rho\omega^2 \widehat{U}(\xi, z) \cdot \boldsymbol{\alpha} - \begin{pmatrix} \hat{\sigma}^1(z, \xi) : \mathcal{A} : \boldsymbol{\beta} \\ \hat{\sigma}^2(z, \xi) : \mathcal{A} : \boldsymbol{\beta} \\ \hat{\sigma}^3(z, \xi) : \mathcal{A} : \boldsymbol{\beta} \end{pmatrix} \right], \qquad \xi \in \Gamma_2, \qquad (81)$$

where

$$\int_{\Gamma_1} \hat{u}^1(z, x)g_1(x) + \hat{u}^2(z, x)g_2(x) + \hat{u}^3(z, x)g_3(x) \, ds_x = \boldsymbol{\alpha},$$

$$\int_{\Gamma_1} \hat{\sigma}^1(z, x)g_1(x) + \hat{\sigma}^2(z, x)g_2(x) + \hat{\sigma}^3(z, x)g_3(x) \, ds_x = \boldsymbol{\beta}. \qquad (82)$$

As can be seen from (81), $\widehat{U}(\xi, z) \cdot \boldsymbol{d}, \xi \in \Gamma_2$ is in the range of $\boldsymbol{F}^\tau$, and one can conclude that (79) is solvable. By use of (81), (82) and a 9×3 stress matrix

$$\widehat{\Sigma}(z, x) = (\hat{\sigma}^1(z, x), \hat{\sigma}^2(z, x), \hat{\sigma}^3(z, x)),$$

(79) can be rewritten as

$$\int_{\Gamma_1} \widehat{U}(z, x) \cdot \boldsymbol{g}_{z,d}^\tau(x) \, ds_x = -\frac{3}{4\pi\tau^3} \frac{1}{\rho\omega^2} \boldsymbol{d},$$

$$\int_{\Gamma_1} \widehat{\Sigma}(z, x) \cdot \boldsymbol{g}_{z,d}^\tau(x) \, ds_x = \mathbf{0}. \qquad (83)$$

In view of (80) which demonstrates that the kernel of $\boldsymbol{F}^\tau$ is degenerate (see [29]), (83) is not uniquely solvable. As a result, a bounded solution of (83) can be specified, e.g., as

$$\boldsymbol{g}_{z,d}^\tau(x) = -\frac{3}{4\pi\tau^3} \frac{1}{\rho\omega^2} ([\overline{\widehat{U}(z, x)}]^T \cdot \boldsymbol{a}_{z,d} + [\overline{\widehat{\Sigma}(z, x)}]^T \cdot \boldsymbol{b}_{z,d}), \qquad (84)$$

where $\boldsymbol{a}_{z,d}$ and $\boldsymbol{b}_{z,d}$ are the solution of the linear algebraic system

$$\left(\int_{\Gamma_1} \widehat{U}(z, x) \cdot [\overline{\widehat{U}(z, x)}]^T \, ds_x \right) \cdot \boldsymbol{a}_{z,d} + \left(\int_{\Gamma_1} \widehat{U}(z, x) \cdot [\overline{\widehat{\Sigma}(z, x)}]^T \, ds_x \right) \cdot \boldsymbol{b}_{z,d} = \boldsymbol{d},$$

$$\left(\int_{\Gamma_1} \widehat{\Sigma}(z, x) \cdot [\overline{\widehat{U}(z, x)}]^T \, ds_x \right) \cdot \boldsymbol{a}_{z,d} + \left(\int_{\Gamma_1} \widehat{\Sigma}(z, x) \cdot [\overline{\widehat{\Sigma}(z, x)}]^T \, ds_x \right) \cdot \boldsymbol{b}_{z,d} = \mathbf{0},$$

characterized by a positive definite coefficient matrix. Now, one can formulate the following result.

Theorem 6.5. *The inverse problem for the elastic-wave reconstruction of a 'small' obstacle $B_\tau(z) \subset \Omega$ with characteristic size $\tau > 0$ is solvable by the linear sampling method. Its solution, $\boldsymbol{g}^\tau(\cdot; z, d) \in L_2(\Gamma_1)$, behaves so that*

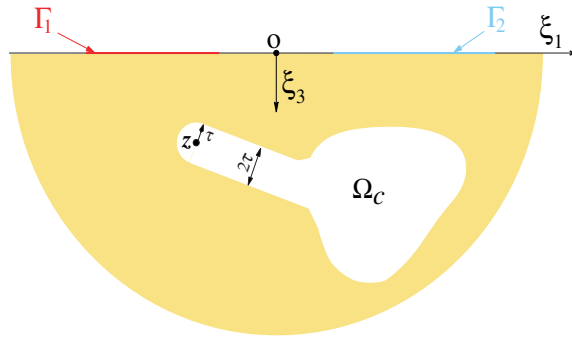$$\lim_{\tau \to 0} \|\boldsymbol{g}^\tau(\cdot; z, d)\|_{L_2(\Gamma_1)} = \infty.$$

Figure 4. Sampling point in the exterior domain

Proof. The assertion of the theorem readily follows from (84) by taking $\tau \to 0$. □

Remark. It was previously shown (see theorem 6.3) that if the sampling point z is inside the scatterer, i.e. $z \in B_\tau(z)$, there exists $g^\tau(\cdot; z, d) \in L_2(\Gamma_1)$ such that $\lim_{z \to y \in \partial B_\tau(z)} \|g^\tau(\cdot; z, d)\|_{L_2(\Gamma_1)} = \infty$. On the other hand, theorem 6.5 states that the norm $\|g^\tau(\cdot; z, d)\|_{L_2(\Gamma_1)}$ becomes unbounded as the boundary $\partial B_\tau(z)$ approaches the sampling point z, i.e. as $\tau = \min_{y \in \partial B_\tau(z)} \|z - y\| \to 0$. Accordingly, theorems 6.3 and 6.5 illustrate the fact that the respective limits are interchangeable.

6.4. Behaviour of the solution in the exterior domain

To provide a comprehensive mathematical basis for the linear sampling method dealing with inverse scattering problems in elastodynamics, the behaviour of the solution to the near-field integral equation (27) when the sampling point lies outside of the scatterer ($z \in \Omega^-$) is the focus of this section. In other words, one has to examine the integral equation

$$(Fg_{z,d})(\xi) = \widehat{U}(\xi, z) \cdot d, \qquad \xi \in \Gamma_2, \quad z \in \Omega^-, \quad d \in \mathbb{R}^3, \quad \|d\| = 1. \tag{85}$$

With the assumption that $g_{z,d} \in L_2(\Gamma_1)$ and that $z \in \Omega^-$ is fixed, it is easy to show that $\widehat{U}(\xi, z) \cdot d, \xi \in \Gamma_2$ is not in the range of F. In particular, the opposite claim that $\widehat{U}(\xi, z) \cdot d, \xi \in \Gamma_2$ is in the range of F contradicts the analyticity of

$$v^S(\xi) = \int_{\Gamma_1} U^S(\xi, x) \cdot g_{z,d}(x) \, ds_x, \qquad \xi \in \Omega^-.$$

In what follows, an approximation of (85) that is solvable in the L_2-sense will be considered instead.

To this end, let $z \in \Omega^-$. With reference to figure 4, consider the perturbed scatterer domain $\widetilde{\Omega}_{C,\tau} = \Omega_C \cup H_\tau \cup B_\tau^+(z)$, where B_τ^+ is a semi-ball of radius $\tau > 0$ centred at z, and H_τ is a cylinder-like domain of radius $\tau > 0$ smoothly connecting Ω_C and $B_\tau^+(z)$. Further, let Γ and $\widetilde{\Gamma}_\tau$ denote the respective boundaries of Ω_C and $\widetilde{\Omega}_{C,\tau}$, so that $\Gamma_\tau = \widetilde{\Gamma}_\tau \setminus (\Gamma \cap \widetilde{\Gamma}_\tau)$ is the 'exposed' boundary of the appendage in figure 4. With these definitions, one may analyse the integral equation

$$\int_{\Gamma_1} \widetilde{U}_\tau^S(\xi, x) \cdot \widetilde{g}_{z,d}^\tau(x) \, ds_x = \widehat{U}(\xi, z) \cdot d,$$

$$\xi \in \Gamma_2, \quad z \in \widetilde{\Omega}_{C,\tau} \subset \Omega, \quad d \in \mathbb{R}^3, \quad \|d\| = 1,$$

introduced as a perturbation of (85), where $\widetilde{U}_\tau^{\mathrm{S}}$ is the scattered tensor induced by $\widetilde{\Omega}_{\mathrm{C},\tau} \subset \Omega$ at $\xi \in \Gamma_2$ due to a unit point source at $x \in \Gamma_1$. On denoting

$$\widetilde{U}_\tau^{\mathrm{S}}(\xi, x) = U^{\mathrm{S}}(\xi, x) + V_\tau^{\mathrm{S}}(\xi, x), \tag{86}$$

where U^{S} is the original (i.e. unperturbed) scattered tensor, one can formulate the following claim.

Theorem 6.6. *Let $z \in \Omega^-$ be fixed, and $d \in \mathbb{R}^3$ with $\|d\| = 1$. Then, for every $\varepsilon > 0$, there exists $\widetilde{g}_{z,d}^\tau \in L_2(\Gamma_1)$, $\tau > 0$, such that*

$$\left\| \int_{\Gamma_1} \left[U^{\mathrm{S}}(\cdot, x) + V_\tau^{\mathrm{S}}(\cdot, x) \right] \cdot \widetilde{g}_{z,d}^\tau(x) \, \mathrm{d}s_x - \widehat{U}(\cdot, z) \cdot d \right\|_{L_2(\Gamma_2)} < \varepsilon, \tag{87}$$

where

$$\lim_{\tau \to 0} V_\tau^{\mathrm{S}}(\cdot, x) = \mathbf{0}, \qquad and \qquad \lim_{\tau \to 0} \left\| \widetilde{g}_{z,d}^\tau \right\|_{L_2(\Gamma_1)} = \infty. \tag{88}$$

Proof. With the assumption that $z \in \widetilde{\Omega}_{\mathrm{C},\tau} \subset \Omega$ is fixed and decomposition (86), one can infer from theorem 6.3 that there exists a solution $\widetilde{g}_{z,d}^\tau \in L_2(\Gamma_1)$ that satisfies the inequality (87). Further, on employing the interchangeability of the limits $z \to y \in \widetilde{\Gamma}_\tau$ and $\tau \to 0$ as examined in section 6.3, it follows from (64) that

$$\lim_{\tau \to 0} \left\| \widetilde{g}_{z,d}^\tau \right\|_{L_2(\Gamma_1)} = \infty.$$

To show that $\lim_{\tau \to 0} V_\tau^{\mathrm{S}}(\cdot, x) = \mathbf{0}$, it is useful to employ an integral representation of the *perturbed* scattered field $\widetilde{U}_\tau^{\mathrm{S}}(\xi, x)$, $\xi \in \Gamma_2$, $x \in \Gamma_1$ corresponding to $\widetilde{\Omega}_{\mathrm{C},\tau}$, i.e.

$$\widetilde{U}_\tau^{\mathrm{S}}(\xi, x) = \int_{\widetilde{\Gamma}_\tau} \left\{ [\widehat{U}(\eta, \xi)]^{\mathrm{T}} \cdot \widetilde{T}_\tau^{\mathrm{S}}(\eta, x) \, \mathrm{d}\Gamma_\eta - [\widehat{T}(\eta, \xi)]^{\mathrm{T}} \cdot \widetilde{U}_\tau^{\mathrm{S}}(\eta, x) \right\} \mathrm{d}\Gamma_\eta. \tag{89}$$

Likewise, one may write

$$U^{\mathrm{S}}(\xi, x) = \int_{\widetilde{\Gamma}_\tau} \{ [\widehat{U}(\eta, \xi)]^{\mathrm{T}} \cdot T^{\mathrm{S}}(\eta, x) \, \mathrm{d}\Gamma_\eta - [\widehat{T}(\eta, \xi)]^{\mathrm{T}} \cdot U^{\mathrm{S}}(\eta, x) \} \, \mathrm{d}\Gamma_\eta, \tag{90}$$

for the *unperturbed* scattered field on the same (perturbed) boundary $\widetilde{\Gamma}_\tau$.

For scattering problems where Ω_{C} (and thus $\widetilde{\Omega}_{\mathrm{C},\tau}$) is a cavity, $T^{\mathrm{S}}(\eta, x) = -\widehat{T}(\eta, x)$, $\eta \in \Gamma$, $x \in \Gamma_1$, and $\widetilde{T}_\tau^{\mathrm{S}}(\eta, x) = -\widehat{T}(\eta, x)$, $\eta \in \widetilde{\Gamma}_\tau$, $x \in \Gamma_1$. On the basis of this result and (89) to (90), one finds that

$$U^{\mathrm{S}}(\xi, x) - \widetilde{U}_\tau^{\mathrm{S}}(\xi, x) = -\int_{\widetilde{\Gamma}_\tau} [\widehat{T}(\eta, \xi)]^{\mathrm{T}} \cdot \left(U^{\mathrm{S}}(\eta, x) - \widetilde{U}_\tau^{\mathrm{S}}(\eta, x) \right) \mathrm{d}\Gamma_\eta + W_\tau^{\mathrm{S}}(\xi, x), \tag{91}$$

where

$$W_\tau^{\mathrm{S}}(\xi, x) = \int_{\Gamma_\tau} [\widehat{U}(\eta, \xi)]^{\mathrm{T}} \cdot (T^{\mathrm{S}}(\eta, x) + \widehat{T}(\eta, x)) \, \mathrm{d}\Gamma_\eta = O(\tau^q),$$

as $\tau \to 0$, $\xi \in \Gamma_2$, $x \in \Gamma_1$ and $q \geqslant 1$. Although the exact value of q is not relevant in this study, it can be shown using the divergence theorem that $q = 2$ for the problem of interest (see also [24]). To examine the behaviour of the residual integral in (91), it is useful to note that the boundary distribution of the *perturbed* scattered field $\widetilde{U}_\tau^{\mathrm{S}}(\eta, x)$ solves the regularized integral equation

$$\widetilde{U}_\tau^{\mathrm{S}}(y, x) + \int_{\widetilde{\Gamma}_\tau} [\widehat{T}(\eta, y)]_1^{\mathrm{T}} \cdot \left(\widetilde{U}_\tau^{\mathrm{S}}(\eta, x) - \widetilde{U}_\tau^{\mathrm{S}}(y, x) \right) \mathrm{d}\Gamma_\eta + \int_{\widetilde{\Gamma}_\tau} [\widehat{T}(\eta, y)]_2^{\mathrm{T}} \cdot \widetilde{U}_\tau^{\mathrm{S}}(\eta, x) \, \mathrm{d}\Gamma_\eta$$

$$= -\int_{\widetilde{\Gamma}_\tau} [\widehat{U}(\eta, y)]^{\mathrm{T}} \cdot \widehat{T}(\eta, x) \, \mathrm{d}\Gamma_\eta, \qquad y \in \widetilde{\Gamma}_\tau, \tag{92}$$

where the traction Green tensor, $\widehat{\boldsymbol{T}}(\boldsymbol{\eta}, \boldsymbol{y}) = [\widehat{\boldsymbol{T}}(\boldsymbol{\eta}, \boldsymbol{y})]_1 + [\widehat{\boldsymbol{T}}(\boldsymbol{\eta}, \boldsymbol{y})]_2$, is decomposed into its singular $[\widehat{\boldsymbol{T}}(\boldsymbol{\eta}, \boldsymbol{y})]_1$ and regular $[\widehat{\boldsymbol{T}}(\boldsymbol{\eta}, \boldsymbol{y})]_2$ parts (see [36]). With reference to $\widetilde{\Gamma}_\tau$, boundary integral equation for the *unperturbed* scattered field $\boldsymbol{U}^{\mathrm{S}}(\boldsymbol{\eta}, \boldsymbol{x})$ can be written as

$$\boldsymbol{U}^{\mathrm{S}}(\boldsymbol{y}, \boldsymbol{x}) + \int_{\widetilde{\Gamma}_\tau} [\widehat{\boldsymbol{T}}(\boldsymbol{\eta}, \boldsymbol{y})]_1^{\mathrm{T}} \cdot (\boldsymbol{U}^{\mathrm{S}}(\boldsymbol{\eta}, \boldsymbol{x}) - \boldsymbol{U}^{\mathrm{S}}(\boldsymbol{y}, \boldsymbol{x}))\, \mathrm{d}\Gamma_\eta + \int_{\widetilde{\Gamma}_\tau} [\widehat{\boldsymbol{T}}(\boldsymbol{\eta}, \boldsymbol{y})]_2^{\mathrm{T}} \cdot \boldsymbol{U}^{\mathrm{S}}(\boldsymbol{\eta}, \boldsymbol{x})\, \mathrm{d}\Gamma_\eta$$

$$= -\int_{\widetilde{\Gamma}_\tau} [\widehat{\boldsymbol{U}}(\boldsymbol{\eta}, \boldsymbol{y})]^{\mathrm{T}} \cdot \widehat{\boldsymbol{T}}(\boldsymbol{\eta}, \boldsymbol{x})\, \mathrm{d}\Gamma_\eta$$

$$+ \int_{\Gamma_\tau} [\widehat{\boldsymbol{U}}(\boldsymbol{\eta}, \boldsymbol{y})]^{\mathrm{T}} \cdot (\widehat{\boldsymbol{T}}(\boldsymbol{\eta}, \boldsymbol{x}) + \boldsymbol{T}^{\mathrm{S}}(\boldsymbol{\eta}, \boldsymbol{x}))\, \mathrm{d}\Gamma_\eta, \qquad \boldsymbol{y} \in \widetilde{\Gamma}_\tau. \tag{93}$$

Here it should be noted that (i) both (elastodynamic) integral equations are by definition well posed, and (ii) all integrands in (92) and (93) are at most weakly singular owing to the assumption that $\widetilde{\boldsymbol{U}}_\tau^{\mathrm{S}}$ and $\boldsymbol{U}^{\mathrm{S}}$ are Hölder continuous. On subtracting (93) from (92), the integral equation for the perturbed scattered field can be recast as

$$\boldsymbol{V}_\tau^{\mathrm{S}}(\boldsymbol{y}, \boldsymbol{x}) + \int_{\widetilde{\Gamma}_\tau} [\widehat{\boldsymbol{T}}(\boldsymbol{\eta}, \boldsymbol{y})]_1^{\mathrm{T}} \cdot \left(\boldsymbol{V}_\tau^{\mathrm{S}}(\boldsymbol{\eta}, \boldsymbol{x}) - \boldsymbol{V}_\tau^{\mathrm{S}}(\boldsymbol{y}, \boldsymbol{x})\right) \mathrm{d}\Gamma_\eta + \int_{\widetilde{\Gamma}_\tau} [\widehat{\boldsymbol{T}}(\boldsymbol{\eta}, \boldsymbol{y})]_2^{\mathrm{T}} \cdot \boldsymbol{V}_\tau^{\mathrm{S}}(\boldsymbol{\eta}, \boldsymbol{x})\, \mathrm{d}\Gamma_\eta$$

$$= -\int_{\Gamma_\tau} [\widehat{\boldsymbol{U}}(\boldsymbol{\eta}, \boldsymbol{y})]^{\mathrm{T}} \cdot (\widehat{\boldsymbol{T}}(\boldsymbol{\eta}, \boldsymbol{x}) + \boldsymbol{T}^{\mathrm{S}}(\boldsymbol{\eta}, \boldsymbol{x}))\, \mathrm{d}\Gamma_\eta, \qquad \boldsymbol{y} \in \widetilde{\Gamma}_\tau, \tag{94}$$

where $\boldsymbol{U}^{\mathrm{S}}$ is assumed to be known beforehand. By virtue of the divergence theorem, it can be shown that the right-hand side of (94) behaves as $O(\tau^2)$ as $\tau \to 0$. As a result, solution of the linear integral equation (94) (which, in view of (92) and (93), constitutes a *well-posed* problem for any $\tau > 0$) exhibits the behaviour

$$\boldsymbol{V}_\tau^{\mathrm{S}}(\boldsymbol{y}, \boldsymbol{x}) = O(\tau^2), \qquad \text{as } \tau \to 0, \quad \boldsymbol{y} \in \widetilde{\Gamma}_\tau, \quad \boldsymbol{x} \in \Gamma_1.$$

By virtue of (91), this result concludes the proof of (88).

For scattering problems where Ω_{C} is an immobile rigid obstacle, (88) can be established using an approach similar to that presented above. For brevity reasons, however, this proof will be omitted. $\qquad\qquad\square$

Remark. To provide further insight into the behaviour of $\boldsymbol{g}_{z,d}$ when $z \in \Omega^-$, it can also be shown using the Tikhonov regularization (see [5] for problems in acoustics) that for every $\varepsilon > 0$ and $\delta > 0$ there exists $\boldsymbol{g}_{z,d}^{\varepsilon,\delta} \in L_2(\Gamma_1)$, such that

$$\left\| \int_{\Gamma_1} \boldsymbol{U}^{\mathrm{S}}(\cdot, \boldsymbol{x}) \cdot \boldsymbol{g}_{z,d}^{\varepsilon,\delta}(\boldsymbol{x})\, \mathrm{d}s_{\boldsymbol{x}} - \widehat{\boldsymbol{U}}(\cdot, \boldsymbol{z}) \cdot \boldsymbol{d} \right\|_{L_2(\Gamma_2)} < \varepsilon + \delta,$$

where

$$\lim_{\delta \to 0} \left\| \boldsymbol{g}_{z,d}^{\varepsilon,\delta} \right\|_{L_2(\Gamma_1)} = \infty.$$

With the result of theorems 6.3, 6.4 and 6.6, it is seen that the function $\|\boldsymbol{g}(\cdot; \boldsymbol{z}, \boldsymbol{d})\|_{L_2(\Gamma_1)}, \boldsymbol{z} \in \Omega$, can be used as an efficient tool for exposing the support of the hidden scatterer Ω_{C} through the region of its bounded values. However, since $\|\boldsymbol{g}(\cdot; \boldsymbol{z}, \boldsymbol{d})\|_{L_2(\Gamma_1)}$ exhibits an unbounded behaviour in Ω^-, it is more convenient to employ $1/\|\boldsymbol{g}(\cdot; \boldsymbol{z}, \boldsymbol{d})\|_{L_2(\Gamma_1)}, \boldsymbol{z} \in \Omega$, as an indicator (i.e. characteristic function) of the hidden scatterer.

Although herein formulated and analysed for near-field elastic waves in a half-space, the linear sampling method derived in this study is also valid for near-field elastic scattering problems in a free space. This can be achieved by replacing the elastodynamic half-space Green function $\hat{\boldsymbol{u}}^k$ by the corresponding free-space fundamental solution [30].
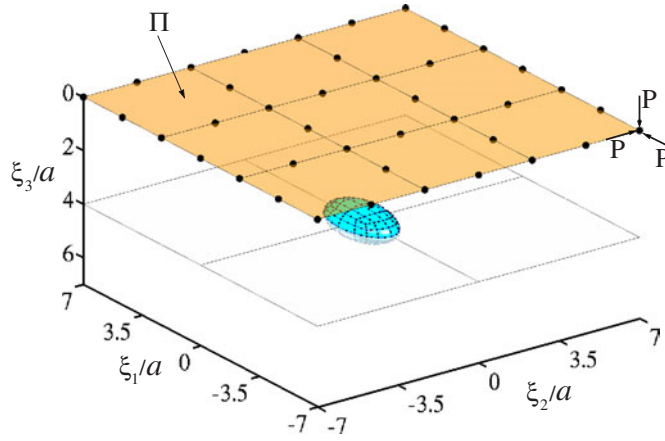
Figure 5. Ellipsoidal cavity and testing configuration in the half-space $\xi_3 > 0$.

7. Results

As elucidated earlier, identification of the support of an obstacle Ω_C hidden in a semi-infinite solid Ω, can be effected by solving the near-field linear integral equation of the first kind (27) in a sampling region $D \subset \Omega$ containing the scatterer. In particular, this process is done by exciting the half-space with a 'fictitious' point source at a *sampling* point $z \in D$ acting in the direction given by a unit vector d, solving (27) for $g(\cdot; z, d)$, and plotting $1/\|g(\cdot; z, d)\|_{L_2(\Gamma_1)}$ for all $z \in D$. More precisely, it was shown via theorems 6.3 through 6.6 that the norm of the density $g_{z,d} = g(\cdot; z, d)$ becomes unbounded whenever $z \notin \Omega_C$. In what follows, the support of Ω_C can be identified by resolving the operator equation

$$F g_{z,d} = b_{z,d} \tag{95}$$

where F is the linear compact operator defined by (31), and $b_{z,d} = \widehat{U}(\cdot, z) \cdot d$. To obtain a stable solution to the ill-posed equation (95), the Tikhonov regularization method [26] is employed in this study wherein the regularized solution of (95) can be found by minimizing the Tikhonov functional

$$J_\alpha(g_{z,d}) = \|F g_{z,d} - b_{z,d}\|^2_{L_2(\Gamma_2)} + \alpha \|g_{z,d}\|^2_{L_2(\Gamma_1)}, \qquad \mathbb{R} \ni \alpha > 0, \tag{96}$$

where the *regularization* parameter α is chosen according to Morozov's discrepancy principle [32].

7.1. Reconstruction of a single-cavity using triaxial seismic excitation

To illustrate the performance of the linear sampling method for near-field elastodynamic inverse problems, the next example deals with the elastic-wave imaging of an ellipsoidal void (the Neumann problem) buried in a semi-infinite solid as depicted in figure 5. With reference to the Cartesian frame, $\{O; \xi_1, \xi_2, \xi_3\}$, the cavity is centred at $(0, 0, 4a)^{\mathrm{T}}$; its semi-axes lengths, aligned with the global coordinate system, are taken as $(1.8a, a, 0.6a)^{\mathrm{T}}$, where a represents the semi-axis in the ξ_2-direction.

On assuming that the source surface Γ_1 and the observation surface Γ_2 coincide (i.e. $\Gamma_1 = \Gamma_2 = \Pi$), the numerical example employs noise-free synthetic data $U^{\mathrm{S}}(\xi, x)$, computed
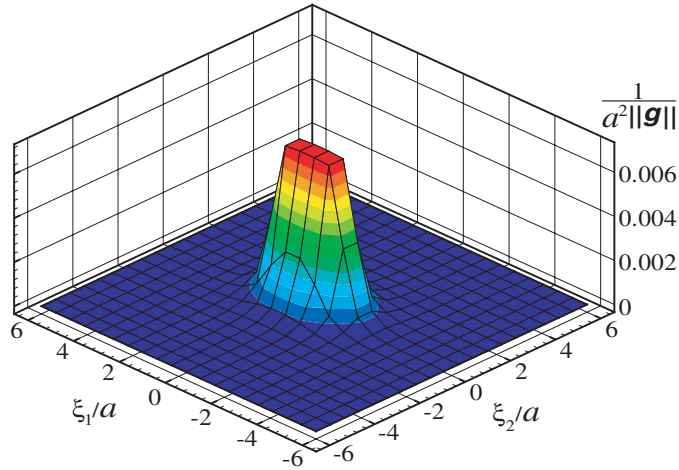
Figure 6. Plot of $1/(a^2\|g(\cdot; z, d)\|_{L_2(\Pi)})$ exposing the 'true' ellipsoidal cavity from triaxial seismic excitation ($\xi_3 = 4a$, $\bar{\omega} = 1.8$, $d = (1, 0, 0)^{\mathrm{T}}$).

using the regularized boundary integral equation [35]. The elastic properties of the half-space and the frequency of excitation are chosen as

$$\mathbf{C} = \frac{3}{2}\mu\mathbf{I}_2 \otimes \mathbf{I}_2 + 2\mu\mathbf{I}_4, \qquad \bar{\omega} = 3.6a\frac{\omega}{\sqrt{\mu/\rho}} = 1.8, \quad \mu > 0. \qquad (97)$$

In the simulation, the cavity is exposed sequentially using 40 source points according to the testing grid shown in figure 5. From each point of the grid, the void is illuminated in sequence using vibratory forces acting in three perpendicular directions (ξ_1, ξ_2 and ξ_3) with respective magnitude $P_1 = P_2 = P_3 = P = 0.2\mu a^2$. For each point source $x \in \Pi$, the noise-free synthetic scattered tensor, $U^{\mathrm{S}}(\xi, x)$, ξ, $x \in \Pi$, is generated at the same (forty) grid points covering the test area $14a \times 14a$ as illustrated in the figure.

With the above problem parameters, the near-field equation (95) is used to compute the density $g_{z,d}$ where the probing point z runs through a rectangular parallelepiped ($12a \times 12a \times 7a$), *a priori* known to contain the scatterer. In the computation of $g_{z,d}$, the right-hand side of (95) is specified according to a 'virtual' point source z with magnitude $P = 0.2\mu a^2$, vibrating with frequency ω in the direction given by the unit vector $d = (1, 0, 0)^{\mathrm{T}}$.

Figure 6 shows the plot of $1/(a^2\|g(\cdot; z, d)\|_{L_2(\Pi)})$ as a function of the probing point z in the horizontal plane $\xi_3 = 4a$ (covering an area of $12a \times 12a$), where $g(\cdot; z, d)$ is computed over a 20×20 grid of uniformly spaced sampling points. As can be seen from the figure, the distribution indicates the support of the hidden scatterer.

Figures 7(a) and (b) depict, respectively, the contour plots of $1/\|(a^2 g(\cdot; z, d)\|_{L_2(\Pi)})$ as a function of the probing point z in the horizontal plane $\xi_3 = 4a$, and in the vertical plane $\xi_1 = 0$. In both horizontal ($12a \times 12a$) and vertical ($12a \times 7a$) planes, a 20×20 grid of uniformly spaced sampling points was used in the numerical evaluation of the density $g(\cdot; z, d)$. As can be seen from the figure, the region of interest (i.e. containing the scatterer) is identified by the regularized sampling method. It should be noted, however, that while the presence of an elliptically shaped object is clearly visible in the horizontal plane from figure 7(a), the reconstruction of the support of the scatterer is somewhat smeared on the vertical plane shown on figure 7(b). This difficulty in the reconstruction on the vertical plane can be associated with (i) the *limited aperture* effect (the surface patch Π subtends a solid angle of only 3.42 sr
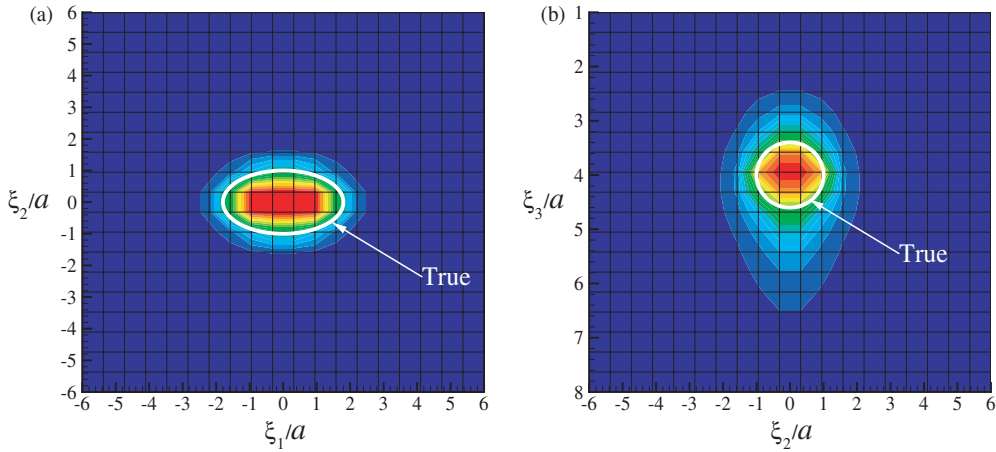
Figure 7. Contour plot of $1/(a^2\|g(\cdot; z, d)\|_{L_2(\Pi)})$ for the identification of an ellipsoidal void using triaxial point source ($\bar{\omega} = 1.8, d = (1, 0, 0)^{\mathrm{T}}$): (a) horizontal plane, $\xi_3 = 4a$ and (b) vertical plane, $\xi_1 = 0$.
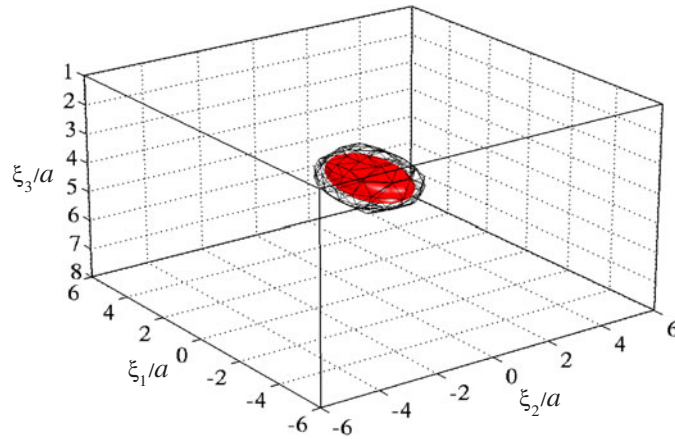
Figure 8. Level surface of $1/(a^2\|g(\cdot; z, d)\|_{L_2(\Pi)})$ in the rectangular box ($12a \times 12a \times 7a$) with level value 10^{-3} ($\bar{\omega} = 1.8, d = (1, 0, 0)^{\mathrm{T}}$).

at the centre of the ellipsoidal cavity), and (ii) the choice of the direction, d, (in this case, $d = (1, 0, 0)^{\mathrm{T}}$) of the point source at the sampling point z (see also [3]).

To provide further insight into the performance of the method, figure 8 illustrates the reconstructed cavity as level set of $1/(a^2\|g(\cdot; z, d)\|_{L_2(\Pi)})$ in the rectangular parallelepiped ($12a \times 12a \times 7a$) with the level value 10^{-3} chosen in accordance to figure 6. In the figure, the true ellipsoidal cavity is also shown inside the level surface.

7.2. Reconstruction of two cavities using triaxial seismic excitation

Motivated by the fact that the near-field equation (95) does not directly involve the boundary of the scatterer, an attempt to identify two isolated ellipsoidal cavities buried in the elastic half-space is undertaken to examine the generality of the linear sampling method. With reference to the Cartesian frame, $\{O; \xi_1, \xi_2, \xi_3\}$, the cavities are centred, respectively, at $(-4a, -2a, 4a)^{\mathrm{T}}$
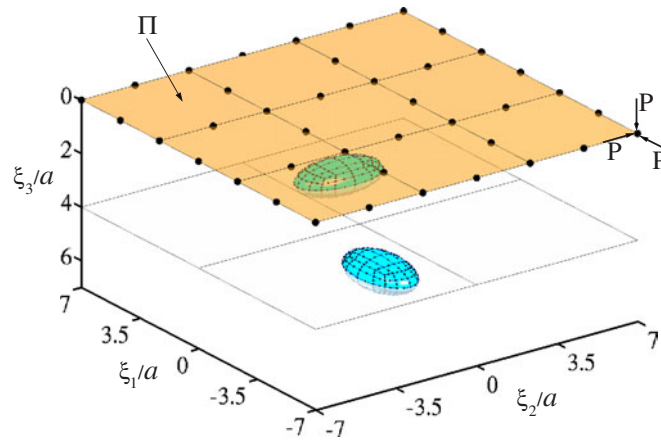
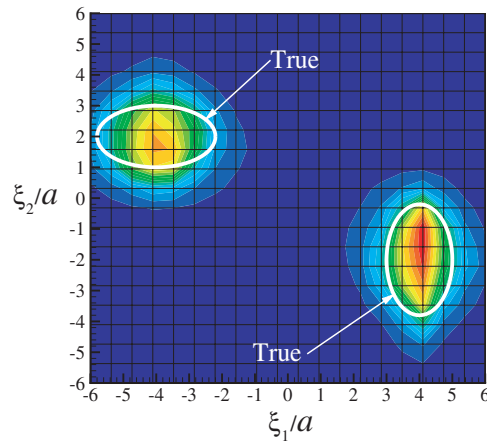**Figure 9.** Ellipsoidal cavities and testing configuration in the half-space $\xi_3 > 0$.

Figure 10. Contour plot of $1/(a^2\|g(\cdot; z, d)\|_{L_2(\Pi)})$ for the reconstruction of an two ellipsoidal cavities using triaxial point source ($\bar{\omega} = 1.8$, $d = (0, 1, 0)^{\mathrm{T}}$): horizontal plane, $\xi_3 = 4a$.

and $(4a, 2a, 4a)^{\mathrm{T}}$ as shown in figure 9. Their semi-axes lengths, aligned with the global coordinate system, are taken, respectively, as $(1.8a, a, 0.6a)^{\mathrm{T}}$ and $(a, 1.8a, 0.6a)^{\mathrm{T}}$.

As in the previous example, the cavities are exposed using 40 point sources with magnitude $P = 0.2\mu a^2$ according to the testing grid depicted in figure 9. The constitutive parameters of the half-space and the frequency of excitation are again chosen according to (97). For every point source $x \in \Pi$, the noise-free scatterer field $U^{\mathrm{S}}(\xi, x)$, $\xi, x \in \Pi$ is evaluated at the same (forty) grid points over the test area $14a \times 14a$ using the regularized boundary integral formulation [35]. With such synthetic data, (95) is solved for the density $g_{z,d}$ at a 20×20 grid of sampling points, uniformly spaced over a $12a \times 12a$ square area in the equatorial plane $\xi_3 = 4a$. In the simulation, a fictitious point source with magnitude $P = 0.2\mu a^2$ and polarization $d = (0, 1, 0)^{\mathrm{T}}$, is specified at every sampling point z.

Figure 10 illustrates the contour plot of $1/(a^2\|g(\cdot; z, d)\|_{L_2(\Pi)})$. The presence of two isolated cavities should be again apparent from the display.

8. Conclusions

In this study, the problem of reconstructing three-dimensional obstacles buried in a semi-infinite solid from near-field, surface seismic measurements is investigated by means of the linear sampling method that is rooted in far-field acoustics. To this end, a three-dimensional inverse analysis of elastic waves scattered by an obstacle in a semi-infinite solid is formulated as a linear integral equation of the first kind whose solution becomes unbounded in the exterior of the hidden scatterer. This unboundedness property of the solution is used to determine the support of the unknown scatterer. For a rigorous approach to the problem, the theoretical foundation of the linear sampling method is systematically extended to near-field elastodynamics in semi-infinite solids, including the necessary existence and uniqueness theorems. Numerical examples indicate that the new technique is capable of effectively identifying subterranean obstacles, both in terms of their location, topology and approximate geometry.

Acknowledgments

References

[1] Achenbach J D 1984 *Wave Propagation in Elastic Solids* (Amsterdam: North-Holland)
[2] Alves C J S and Kress R 2002 On the far-field operator in elastic obstacle scattering *IMA J. Appl. Math.* **67** 1–21
[3] Arens T 2001 Linear sampling methods for 2D inverse elastic wave scattering *Inverse Problems* **17** 1445–64
[4] Charalambopoulos A, Gintides D and Kiriaki K 2002 The linear sampling method for the transmission problem in three-dimensional linear elasticity *Inverse Problems* **18** 547–58
[5] Cakoni F and Colton D 2003 On the mathematical basis of the linear sampling method *Georgian Math. J.* **10** 411–25 (Kupradze's special issue)
[6] Colton D 1980 *Analytic Theory of Partial Differential Equations* (London: Pitman)
[7] Colton D and Kirsch A 1996 A simple method for solving inverse scattering problems in the resonance region *Inverse Problems* **12** 383–93
[8] Colton D, Piana M and Potthast R 1997 A simple method using Morozov's discrepancy principle for solving inverse scattering problems *Inverse Problems* **13** 1477–93
[9] Colton D and Kress R 1998 *Inverse Acoustic and Electromagnetic Scattering Theory* (Berlin: Springer)
[10] Colton D and Monk P 1998 Linear sampling method for the detection of leukemia using microwaves *SIAM J. Appl. Math.* **58** 926–41
[11] Colton D and Monk P 1999 Linear sampling method for the detection of leukemia using microwaves II *SIAM J. Appl. Math.* **60** 241–55
[12] Colton D, Giebermann K and Monk P 2000 Regularized sampling method for solving three-dimensional inverse scattering problems *SIAM J. Sci. Comput.* **21** 2316–30
[13] Colton D, Coyle J and Monk P 2000 Recent developments in inverse acoustic scattering theory *SIAM Rev.* **42** 369–414
[14] Colton D and Kress R 2001 On the denseness of Herglotz wave functions and electromagnetic Herglotz pairs in Sobolev spaces *Math. Methods Appl. Sci.* **24** 1289–303
[15] Coyle J 2000 Locating the support of objects contained in a two-layered background medium in two dimensions *Inverse Problems* **16** 275–92
[16] Dassios G and Rigou Z 1995 Elastic Herglotz functions *SIAM J. Appl. Math.* **55** 1345–61
[17] Garabedian P R 1998 *Partial Differential Equations* (Providence, RI: AMS Chelsea)
[18] Gintides D and Kiriaki K 1992 On the continuity dependence of elastic scattering amplitudes upon the shape of the scatterer *Inverse Problems* **8** 95–118
[19] Gintides D 1999 The inverse scattering problem in three-dimensional elasticity *Z. Angew. Math. Mech.* **79** 675–84

[20] Gintides D and Kiriaki K 2001 The far-field equations in linear elasticity–an inversion scheme *Z. Angew. Math. Mech.* **81** 305–16

[21] Graff K F 1991 *Wave Motion in Elastic Solids* (New York: Dover)

[22] Guzina B B and Pak R Y S 2001 On the analysis of wave motions in a multi-layered solid *Quart. J. Mech. Appl. Math.* **54** 13–37

[23] Guzina B B, Nintcheu Fata S and Bonnet M 2003 On the stress-wave imaging of cavities in a semi-infinite solid *Int. J. Solids Struct.* **40** 1505–23

[24] Guzina B B and Bonnet M 2004 Topological derivative for the inverse scattering of elastic waves *Quart. J. Mech. Appl. Math.* **57** 161–79

[25] Haddar H and Monk P 2002 The linear sampling method for solving the electromagnetic inverse medium problem *Inverse Problems* **18** 891–906

[26] Kirsch A 1996 *An Introduction to the Mathematical Theory of Inverse Problems* (Berlin: Springer)

[27] Knops R J and Payne L E 1971 *Uniqueness Theorems in Linear Elasticity* (Berlin: Springer)

[28] Kress R 1996 Inverse elastic scattering from a crack *Inverse Problems* **12** 667–84

[29] Kress R 1999 *Linear Integral Equation* (Berlin: Springer)

[30] Kupradze V D 1979 *Three-Dimensional Problems of the Mathematical Theory of Elasticity and Thermoelasticity* (Amsterdam: North-Holland)

[31] McLean W 2000 *Strongly Elliptic Systems and Boundary Integral Equations* (Cambridge: Cambridge University Press)

[32] Morozov V A 1984 *Methods for Solving Incorrectly Posed Problems* (Berlin: Springer)

[33] Nédélec J C 2001 *Acoustic and Electromagnetic Equations* (Berlin: Springer)

[34] Nintcheu Fata S 2003 3D Subterranean imaging via elastic waves *PhD Thesis* University of Minnesota

[35] Nintcheu Fata S, Guzina B B and Bonnet M 2003 Computational framework for the BIE solution to inverse scattering problems in elastodynamics *Comp. Mech.* **32** 370–80

[36] Pak R Y S and Guzina B B 1999 Seismic soil-structure interaction analysis by direct boundary element methods *Int. J. Solids Struct.* **36** 4743–66

[37] Pelekanos G and Sevroglou V 2003 Inverse scattering by penetrable objects in two-dimensional elastodynamics *J. Comput. Appl. Math.* **151** 129–40

[38] Rus G and Gallego R 2002 Optimization algorithms for identification inverse problems with the boundary element method *Eng. Anal. Bound. Elem.* **26** 315–27